



# Oxidative testicular injury: effect of L-leucine on redox, cholinergic and purinergic dysfunctions, and dysregulated metabolic pathways

Ochuko L. Erukainure<sup>1</sup> · Olubunmi Atolani<sup>3</sup> · Priyanka Banerjee<sup>4</sup> · Renata Abel<sup>4,5</sup> · Ofentse J. Pooe<sup>2</sup> · Oluyomi S. Adeyemi<sup>6</sup> · Robert Preissner<sup>4</sup> · Chika I. Chukwuma<sup>8</sup> · Neil A. Koorbanally<sup>7</sup> · Md. Shahidul Islam<sup>2</sup>

Received: 24 July 2020 / Accepted: 2 February 2021 / Published online: 14 February 2021  
© The Author(s), under exclusive licence to Springer-Verlag GmbH, AT part of Springer Nature 2021

## Abstract

The antioxidant and anti-proinflammatory activities of L-leucine were investigated on oxidative testicular injury, *ex vivo*. *In vitro* analysis revealed L-leucine to be a potent scavenger of free radicals, while inhibiting acetylcholinesterase activity. Oxidative injury was induced in testicular tissues using FeSO<sub>4</sub>. Treatment with L-leucine led to depletion of oxidative-induced elevated levels of NO, MDA, and myeloperoxidase activity, with concomitant elevation of reduced glutathione and non-protein thiol levels, SOD and catalase activities. L-leucine caused a significant ( $p < 0.05$ ) alteration of oxidative-elevated acetylcholinesterase and chymotrypsin activities, while concomitantly elevating the activities of ATPase, ENTPDase and 5'-nucleotidase. L-leucine conferred a protective effect against oxidative induced DNA damage. Molecular docking revealed molecular interactions with COX-2, IL-1 beta and iNOS. Treatment with L-leucine led to restoration of oxidative depleted ascorbic acid-2-sulfate, with concomitant depletion of the oxidative induced metabolites: D-4-Hydroxy-2-oxoglutarate, L-cystine, adenosine triphosphate, maleylacetoacetic acid, cholesteryl ester, and 6-Hydroxy flavin adenine dinucleotide. Treatment with L-leucine reactivated glycolysis while concomitantly deactivating oxidative-induced citrate cycle and increasing the impact-fold of purine metabolism pathway. L-leucine was predicted not to be an inhibitor of CYP1A2, CYP2C19, CYP2C9, CYP2D6, and CYP3A4, with a predicted LD<sub>50</sub> value of 5000 mg/Kg and toxicity class of 5. Additionally, L-leucine showed little or no *in vitro* cytotoxicity in mammalian cells. These results suggest the therapeutic potentials of L-leucine on oxidative testicular injury, as evident by its ability to attenuate oxidative stress and proinflammation, while stalling cholinergic dysfunction and modulating nucleotide hydrolysis; as well as modulate oxidative dysregulated metabolites and their pathways.

**Keywords** Amino acids · Antioxidants · L-leucine · Medicinal biochemistry · Proinflammation · Testicular dysfunction

Handling editor: S. S. Gross.

✉ Ochuko L. Erukainure  
loreks@yahoo.co.uk

✉ Olubunmi Atolani  
tolanventure@gmail.com

<sup>1</sup> Department of Pharmacology, School of Clinical Medicine, Faculty of Health Sciences, University of the Free State, Bloemfontein 9301, South Africa

<sup>2</sup> Department of Biochemistry, School of Life Sciences, University of KwaZulu-Natal, Westville Campus, Durban 4000, South Africa

<sup>3</sup> Department of Chemistry, University of Ilorin, Ilorin, Nigeria

<sup>4</sup> Structural Bioinformatics Group, Institute for Physiology, Charité – University Medicine Berlin, Berlin, Germany

<sup>5</sup> Department of Pharmaceutical Biology, Medical University of Wroclaw, Borowska 211, 50-556 Wroclaw, Poland

<sup>6</sup> Department of Biochemistry, Landmark University, Omu-Aran, Nigeria

<sup>7</sup> School of Chemistry and Physics, University of KwaZulu-Natal, Westville Campus, Durban 4000, South Africa

<sup>8</sup> Center for Quality of Health and Living, Faculty of Health Sciences, Central University of Technology, Bloemfontein 9301, South Africa

## Introduction

Oxidative stress has been recognized as one of the main stimuli that triggers the pathogenesis and progression of testicular dysfunction (Erukainure et al. 2019b). This can be attributed to the high concentration of unsaturated fatty acids in the testes and sperm cells, which are susceptible to peroxidative damage (Aitken and Roman 2008). The testes are endowed with an array of antioxidant systems of both enzymatic and nonenzymatic constituents. However, the antioxidant system is compromised in the presence excessive free radicals, leading to oxidative stress which is detrimental to male fertility (Erukainure et al. 2012; Obode et al. 2015). Testicular inflammation has also been implicated in the pathogenesis of testicular oxidative damage, leading to decreased testosterone production and spermatogenesis (Guazzone et al. 2009; Reddy et al. 2006). Studies have reported concomitant decreased antioxidant activities and increase in the proinflammatory cytokines, iNOS, IL-1 $\beta$ , and COX-2 (Reddy et al. 2006). Increase in these proinflammatory cytokines causes release of large volumes of O $_2^-$  and H $_2$ O $_2$ , thus suppressing the testicular antioxidant system (Abd-Allah et al. 2009). Cholinergic proteins play important roles in testicular functions and fertility, as their expressions have been reported in Leydig and Sertoli cells (Lucas et al. 2004; Mor and Soreq 2011). Acetylcholine, one of the common cholinergic proteins has also been reported to regulate the functions of Leydig cells, as its expression is exacerbated in the differentiation and maturation of Leydig cell (Ge et al. 2005; Mor and Soreq 2011). Reduced testicular acetylcholine level demonstrated by increased acetylcholinesterase activity has been implicated in the testicular dysfunction (Akomolafe et al. 2017).

Testicular alterations in the endogenous signaling nucleotide, adenosine has been implicated in testicular function and fertility (Burnstock 2014; Gorodeski 2015). It is produced by purinergic enzymatic phospho-hydrolysis of Adenosine triphosphate (ATP) and Adenosine monophosphate (AMP) (Akinyemi et al. 2017; Bagatini et al. 2018). ATP and adenosine have been reported for their ability to stimulate capacitation and fertilization potential of sperm, with the latter stimulating sperm motility (Gorodeski 2015). Anaerobic glycolysis and oxidative phosphorylation are the main metabolic pathways for ATP production in sperm cells, with the former being the predominant (Tourmente et al. 2015).

Aside nutrition, the role of nutrients in the management and treatment of various ailments and diseases are well documented. This corroborates with the emergence of functional foods and nutraceuticals as alternative treatment for various diseases (Gul et al. 2016). Of interest are the

essential amino acids (EAA). Their deficiency has been associated with depressed growth in animals (Anthony et al. 2001). Anthony et al. (2001) further demonstrated that EAA deficiency inhibits mRNA translation of ribosomal proteins in rats' liver. Their anti-inflammatory activities have been demonstrated in both preclinical and clinical studies, with L-leucine being the most prominent (Lee et al. 2017; Nicastro et al. 2017; Saxena et al. 1984).

L-leucine is one of the nine essential amino acids. It is a recognized activator of the mammalian target of rapamycin (mTOR) which regulates cell growth and several aspects of metabolism such as regulation of gene transcription and protein synthesis in pancreatic  $\beta$  cells (Pedroso et al. 2015; Yang et al. 2010). Its anti-inflammatory activity has been demonstrated in healthy volunteers (Nicastro et al. 2017). Its ability to modulate skeletal muscle remodeling has been attributed to its modulatory effect on muscular inflammation (Nicastro et al. 2012). Thus, making it a potential dietary supplement and/or nutraceutical for the treatment and management of several metabolic diseases.

However, there are limited reports on the protective effect of L-leucine against testicular toxicity. Thus, this study was aimed at investigating the protective effect of L-leucine on oxidative stress, cholinergic and purinergic dysfunctions, and dysregulated metabolic pathways in oxidative testicular injury using, *ex vivo*. Its anti-proinflammatory activity and protective effect against DNA damage were investigated using *in vitro* and *in silico* models.

## Materials and methods

### L-leucine

L-leucine (Sigma-Aldrich) was purchased from Bristol Scientific Company, Lagos, Nigeria.

A 1 mg/mL stock solution of L-leucine was prepared in distilled water. From the stock solution, different concentrations ranging from 10 to 50  $\mu$ g/mL and 15–240  $\mu$ g/mL were prepared for *in vitro* and *ex vivo* activities, respectively.

### In vitro activities

#### Determination of antioxidant activity using the DPPH free radical scavenging assay

The 2,2-diphenyl-1-picrylhydrazyl (DPPH) spectrophotometric assay was carried out following standard procedure (Atolani and Olatunji 2016; Atolani et al. 2012). The DPPH free radical reagent was prepared and kept in dark bottle in the refrigerator. The L-leucine was prepared in triplicate in 10–50  $\mu$ g/mL concentrations. 1 mL DPPH solution was added to all samples shaken together and immediately

incubated in the dark for 30 min. The absorbance value was measured at 517 nm. Blank experiment was also carried out to determine the absorbance of DPPH before interacting with the sample. The decreasing absorbance of the DPPH solution was used as an indication of the DPPH radical scavenging activity of the samples. The radical scavenging activity was calculated using the equation:

$$\%AA = 100 \times [(Abs_{\text{control}} - Abs_{\text{sample}})] / (Abs_{\text{control}})$$

where %AA indicates percentage antioxidant activity, while  $Abs_{\text{control}}$  and  $Abs_{\text{sample}}$  were the absorbance of the control and sample at 517 nm, respectively. Results were expressed as mean values  $\pm$  standard error of mean (SEM) of triplicate determinations. The  $IC_{50}$  was determined on GraphPad Prism 6 software (San Diego, USA) through a non-regression analysis. The  $IC_{50}$  was taken as the concentration of sample that scavenged fifty percent of the DPPH radicals.

#### Determination of antioxidant activity using the ABTS free radical scavenging assay

The 2,2'-azinobis-3-ethylbenzothiazoline-6-sulfonate, ABTS radical cation decolorization assay based on the scavenging of  $ABTS^{\bullet+}$  radicals by antioxidants component of the L-Leucin was used. The assay follows standard procedure (Atolani et al. 2013), with slight modifications. ABTS reagent was first dissolved in deionized water to reach a concentration 7 mM and the solution of 2.45 mM potassium persulfate freshly prepared was mixed with it at ratio of 1:1 and kept in the dark for 24 h. The ABTS solution was then diluted in aqueous methanol with a ratio of 1:25. A volume of 20  $\mu$ L (diluted 1:10) of samples was added to 2 mL of  $ABTS^{\bullet+}$  solution, and the mixture was kept at a standard temperature of 30 °C. The absorbance was measured at 734 nm at 10 min after initial mixing. All analyses were determined in triplicate. The ABTS antioxidant activity (AA) was calculated using the expression:

$$AA = 100 \times [(Abs_{\text{control}} - Abs_{\text{sample}})] / (Abs_{\text{control}})$$

where  $Abs_{\text{control}}$  and  $Abs_{\text{sample}}$  are the absorbances of the control and the samples, respectively.

#### Determination of acetylcholinesterase (AChE) inhibitory activity

The ability of L-leucine to inhibit the acetylcholinesterase enzyme from breaking down acetylcholine was evaluated using following standard procedure with slight modifications (Salles et al. 2003). The assay mixture was made up of 200  $\mu$ L Tris-HCl 50 mM (pH 8.0) and 0.1% BSA buffer. 100  $\mu$ L leucin with final concentration: 100  $\mu$ g  $mL^{-1}$  was dissolved in buffer-MeOH (10%) and 100  $\mu$ L of AChE

(0.22 U  $mL^{-1}$ ). The mixture was incubated at room temperature for 2 min before the addition of 500  $\mu$ L of DTNB (5,5'-dithiobis-2-nitrobenzoic acid) (3 mM) and 100  $\mu$ L of substrate acetylthiocholine iodide (ATCI) (15 mM). The developing yellow colour was measured at 405 nm after 4 min. Galantamine was used as positive control at a final concentration of 0.2  $\mu$ g  $mL^{-1}$  in the assay mixture. AChE inhibitory activity was expressed as percentage inhibition of AChE, calculated as  $(1-B/A) \times 100$ , where A is the change in absorbance of the assay without L-leucine ( $Abs_{\text{with enzyme}} - Abs_{\text{without enzyme}}$ ) and B is the change in absorbance of the assay with leucin ( $Abs_{\text{with enzyme}} - Abs_{\text{without enzyme}}$ ).

#### Animals

Three male albino rats (Sprague Dawley strain) weighing 200–250 g were obtained from the Biomedical Research Unit (BRU), University of KwaZulu-Natal, Durban, South Africa. The rats were fasted overnight and were euthanized with halothane. Testes were collected from each animal, rinsed in 0.9% NaCl solution and homogenized in sodium phosphate buffer (50 mM; pH 7.5; with 10% Triton X-100). The homogenized tissues were centrifuged at 22,000 $\times$  g at 4 °C for 10 min (Salau et al. 2020). The supernatants were collected in 2 mL Eppendorf tube and stored at – 4 °C for ex vivo studies.

The approved guidelines of the Animal Ethics Committee of the University of KwaZulu-Natal, Durban, South Africa (Protocol approval number: AREC/020/017D) were duly followed.

#### Ex vivo activities

A 100  $\mu$ L aliquot from each prepared concentration of L-leucine (15–250  $\mu$ g/mL) and the standard drug, gallic acid were incubated with 100  $\mu$ L of testicular tissue homogenates and 30  $\mu$ L of 0.1 mM  $FeSO_4$  at 37 °C for 30 min. Tissues incubated without L-leucine or gallic acid served as negative control (untreated). While tissues not subjected to any incubation served as positive control (normal).

#### Oxidative stress biomarkers

The incubated samples were analyzed for oxidative biomarkers which cover for reduced glutathione (GSH) (Ellman 1959) and non-protein thiol (Adefegha et al. 2017; Habig et al. 1974) levels, catalase (Aebi 1984) and superoxide dismutase (SOD) (Kakkar et al. 1984) activities, and malondialdehyde (MDA) level (Chowdhury and Soulsby 2002).

### Determination of GSH levels

The samples were deproteinized with an equal volume of 10% TCA and then centrifuged at 5000 rpm for 5 min at 25 °C. Aliquot (200 µL) of the supernatant was thereafter pipetted into a 96 well plate, 50 µL of Ellman reagent was then added and the mixture was allowed to stand for 5 min. Absorbance was read at 415 nm. The GSH level was then extrapolated from a standard curve of plotted GSH concentrations.

### Determination of SOD activities

The assay was based on the principle of 6-hydroxydopamine (6-HD) being oxidized by H<sub>2</sub>O<sub>2</sub> from SOD catalyzed dismutation of O<sub>2</sub><sup>•-</sup>, which produces a colored product. Briefly, 15 µL of the supernatants were dissolved in 170 µL of 0.1 mM diethylenetriaminepentaacetic acid (DETAPAC) in a 96-well plate. 15 µL of 1.6 mM 6-HD was then added to the reaction mixture. Absorbance was read at 492 nm for 5 min at 1-min interval.

### Determination of catalase activity

Catalase activity was determined based on the measurement of decreased absorbance of test samples due to H<sub>2</sub>O<sub>2</sub> decomposition. 340 µL of 50 mM sodium phosphate buffer (pH 7.0) was mixed with 10 µL of the samples. Thereafter, 150 µL of 2 M H<sub>2</sub>O<sub>2</sub> was added to the mixture. Absorbance was read at 240 nm for 3 min at 1-min interval.

### Determination of MDA levels

One hundred microliters of the samples were mixed with 100 µL of 8.1% SDS solution, 375 µL of 20% acetic acid, 1 mL of 0.25% thiobarbituric acid (TBA), and 425 µL of distilled water. The reaction mixture was heated at 95 °C for 1 h in a water bath. Thereafter, 200 µL of the heated mixture was pipetted into 96-well plate and absorbance read at 532 nm. MDA levels were extrapolated from a standard curve of plotted standard MDA concentrations.

### Determination of non-protein thiol group (NPSH) levels

Two hundred microliters of the samples were deproteinized with 10% triton, vortexed and allowed to stand for 10 min. 200 µL of 20% TCA was then added, vortexed and centrifuged at 4000 rpm for 10 min at 4 °C. 50 µL of Ellman's reagent was then added to 100 µL of the supernatant and incubated for 1 h at room temperature. Absorbance was read

at 412 nm. NPSH levels were extrapolated from a standard curve of cysteine.

### Proinflammation

The proinflammatory biomarkers were determined by analyzing the samples for nitric oxide (NO) (Erukainure et al. 2019a) and myeloperoxidase activity (Granell et al. 2003), with slight modifications.

### Determination of Nitric Oxide (NO) Level

The NO levels of the testicular tissues were determined using the Griess method with slight modifications. 100 µL of the samples or distilled water (blank) and was incubated with an equal volume of Griess reagent for 30 min at 25 °C in the dark. Absorbance was read at 548 nm.

### Determination of myeloperoxidase activity

One hundred microliters of the samples were incubated with 100 µL of 5 mM KCl and 25 µL of 2 M H<sub>2</sub>O<sub>2</sub> for 10 min. Thereafter, 50 µL of 1.25% ammonium molybdate was added to reaction mixture and allowed to stand for 5 min. Absorbance was read at 405 nm.

### Determination of purinergic enzymes activities

This was carried out by determining the ATPase (Adewoye et al. 2000; Erukainure et al. 2017a), ENTPDase (Ademiluyi et al. 2016; Schetinger et al. 2007) and 5'nucleotidase (5'NT) (Heymann et al. 1984) activities in the testicular tissues.

### Determination of ATPase activity

Two hundred microliters of the tissue samples were incubated with 200 µL of 5 mM KCl, 1300 µL of 0.1 M Tris-HCl buffer, and 40 µL of 50 mM ATP in a shaker for 30 min at 37 °C. 1 mL of distilled water and 1.25% ammonium molybdate were then added to stop the reaction. The reaction mixture was further incubated with 1 mL of freshly prepared 9% ascorbic acid for 30 min at 25 °C. Absorbance was read at 660 nm.

### Determination of ENTPDase activity

Twenty microliters of the tissue samples were incubated with 200 µL of the reaction buffer (1.5 mM CaCl<sub>2</sub>, 5 mM KCl, 0.1 mM EDTA, 10 mM glucose, 225 mM sucrose and 45 mM Tris-HCl) for 10 min at 37 °C. The reaction mixture was further incubated for 20 min at 37 °C after the addition of 20 µL of 50 mM ATP. The reaction was stopped with

200  $\mu\text{L}$  of 10% TCA. The reaction mixture was incubated for 10 min in ice and absorbance read at 600 nm.

### Determination of 5' nucleotidase activity

Briefly, 20  $\mu\text{L}$  of the tissue sample was incubated with 100  $\mu\text{L}$  10 mM  $\text{MgSO}_4$  and 100 mM Tris-HCl buffer, pH 7.5 for 10 min at 37 °C. 2 mM AMP was added to the reaction mixture and further incubated for 10 min at 37 °C. The reaction was stopped with 200  $\mu\text{L}$  of 10% TCA and incubated in ice for 10 min. Absorbance was read at 600 nm.

### Acetylcholinesterase activity

The acetylcholinesterase activity of the tissue samples were determined using the Ellman's method (Ellman et al. 1961). Briefly, 20  $\mu\text{L}$  of the samples were incubated with 10  $\mu\text{L}$  of 3.3 mM Ellman's reagent (pH 7.0) and 50  $\mu\text{L}$  of 0.1 M phosphate buffer (pH 8) for 20 min at 25 °C. 10  $\mu\text{L}$  of 0.05 M acetylcholine iodide was thereafter added to the reaction mixture and absorbance read at 412 nm at 3-min intervals.

### Determination of proteolytic activity

This was carried out by determining the  $\alpha$ -chymotrypsin activity of the tissue samples according to a previously reported method (Saleem et al. 2016), with slight modifications. Briefly, 15  $\mu\text{L}$  of the tissue sample was incubated with 60  $\mu\text{L}$  Tris-HCl buffer (50 mM pH 7.6) at 37 °C for 20 min. The reaction was then initiated by adding 15  $\mu\text{L}$  1.3 mM N-succinyl phenyl-alanine-P-nitroanilide. The reaction mixture was incubated at 37 °C for 30 min, and absorbance read at 410 nm.

### Metabolite extraction and profiling

Equal volumes (100 mL) of L-leucine (240  $\mu\text{g}/\text{mL}$ ) and testicular tissue homogenate were incubated with 30  $\mu\text{L}$  of 0.1 mM  $\text{FeSO}_4$  at 37 °C overnight.

Metabolites were extracted from the incubated samples using previous described protocol (Chan et al. 2013) with slight modifications as described (Erukainure et al. 2017b). The extracted metabolites were subjected to LC-MS analysis using Shimadzu LCMS-2020 Single Quadrupole Liquid Chromatograph Mass Spectrometer (LC-MS) by injecting directly into the machine via a loop. The operating parameters were:

Stop time: 4 min; Photodiode Array (PDA) sampling frequency: 1.5625 Hz; Operating mode: low pressure gradient; Pump A: LC-2030 Pump; Mobile Phase A and B: water and methanol, respectively; Flow rate: 0.200 mL/min; Start and End wavelengths: 190 and 800 nm, respectively; Cell Temp.: 40 °C; Start and End time: 0.00 and 4.00 min, respectively;

acquisition mode: Scan; Scan Speed: 1667 u/s; polarity: positive; event time: 1.00 s; detector voltage: + 1.00 kV; Threshold: 0; Start and End m/z: 50.00 and 1700.00, respectively.

The metabolites were identified by direct search of mass spectral (MS) data with the Human Metabolome Database (Wishart et al. 2013).

### Metabolic pathway analysis

The metabolic pathway analysis was employed in identifying the most relevant metabolic pathways involved in the therapeutic effect of L-leucine on oxidative testicular injury using the MetaboAnalyst 4.0 (Chong et al. 2018). Metabolites showing significant changes were mapped via the Kyoto Encyclopedia of Genes and Genomes (KEGG) pathways using Human Metabolome Database numbers.

### DNA nicking assay

To evaluate the DNA nicking protective role of leucine, plasmid DNA was incubated in the presence  $\text{FeSO}_4$ , and increasing concentrations of leucine or gallic acid (known antioxidant control) according to a previous modified method (Leba et al. 2014; Luo et al. 1994). The reaction mixture was made as follow; 5  $\mu\text{L}$  of pET151/D-TOPO DNA (150  $\mu\text{g}/\mu\text{L}$ ), mixed with 2  $\mu\text{L}$  of  $\text{FeSO}_4$  (100 mM) and variable concentrations of leucine (0.005–5 mg/mL, respectively). Gallic acid solution was used as DNA protection control for this assay. The reaction mixture was made-up to a 20  $\mu\text{L}$  total volume with distilled water. The mixture was incubated for 30 min at 21 °C. Addition of 5  $\mu\text{L}$  of the binding dye (bromophenol blue; 0.25% composed of 50% glycerol) were followed immediately after the incubation period. The samples were then resolved by agarose gel electrophoresis (0.8%) and stained by the addition of ethidium bromide. Electrophoretic mobility of the agarose gel composition was carried out for 60 min at 90 V and viewed using the G:BOX F3 Gene System image.

### Cell viability assays

Human foreskin fibroblast (HFF) cells were maintained in DMEM (Nissui, Tokyo, Japan) supplemented with GlutaMAX™-I (Gibco, Invitrogen, UK), 10% (v/v) fetal calf serum (FCS; Gibco, Invitrogen, UK), and penicillin and streptomycin (100 U/mL; Biowhittaker, UK) at 37 °C and 5%  $\text{CO}_2$  atmosphere. At confluence, cells were trypsinized and resuspended to the desired cell density. The cells were seeded onto plates at a density of  $1 \times 10^4$  cells per well and incubated for 72 h followed by treatment with various concentrations (between 0.1 and 2.5 mg/mL) of leucine diluted in the culture medium. Culture medium not containing L-leucine was added to the control well and the medium

only well was used to correct for background signal. Staurosporine (1  $\mu\text{M}$ ) was included as positive control. The treated cells were incubated for 72 h before and thereafter the cell viability was determined using the CellTitre-Aqueous One Solution proliferation assay kit (Promega, Madison, USA). Briefly, the well plate and its contents were equilibrated to room temperature. Then, 20  $\mu\text{L}$  of the CellTitre-Aqueous One reagent was added to each well. The contents were briefly mixed on an orbital shaker and then incubated at 37 °C in a 5%  $\text{CO}_2$  atmosphere for 1–4 h. The absorbance signal was recorded at 490 nm using a microplate reader (MTP 500; Corona Electric, Hitachinaka Japan).

## Computational docking

### Molecular docking of DNA with L-leucine

Molecular docking of DNA with leucine was performed with GOLD 5.7.1 software. The PDB file of DNA sequences (5'-CGACTAGTCG-3') was downloaded from RCSB Protein Data Bank (PDB code 1RMX). The original ligand and water molecules were removed from the sequence. Binding site was defined based on protocol presented in the study (Anthony et al. 2004; Shukla et al. 2019) and the final protocol for the docking was designed based on the successful re-docking of reported ligand (isopropyl-thiazole) into DNA. The number of best poses was set to 10 and Gold Score scoring function was used to rank the docked ligand. Best docking poses were chosen based on docking score and visual inspections of the receptor-ligand interactions using Accelys, Discovery Studios software 4.1.

### Molecular docking of L-leucine with IL- $\beta$ , COX-2 and iNOS

The promising in vitro anti-inflammatory activity of L-leucine encouraged us to perform molecular docking studies to establish and understand the L-leucine-Pro-inflammatory cytokines and their inducible proteins. Pro-inflammatory cytokine like Interleukin 1 beta (IL1- $\beta$ ) inflammatory-cytokines inducible proteins such as cyclooxygenase-2 (COX-2) and Inducible Nitric Oxide Synthase (iNOS) were chosen for this study.

**Dataset** For this study, the crystal structures of COX-2 (PDB code: 5F19), IL1- $\beta$  (PDB code: 4GAF) and iNOS (PDB code: 1NSI) enzymes complexes were selected and downloaded from the Protein Data Bank (Berman et al. 2000). The data set was structurally processed using Discovery Studio, software version 4.1.

**Docking protocol** For the prediction of possible molecular mechanism involved, molecular docking was conducted using the three-dimensional X-ray crystals pre-processed

and curated (e.g., removal of water, addition of explicit hydrogen) using the Protein Preparation Wizard from the Gold Suite (Jones et al. 1997). The histidine protonation states were determined and fixed in the protein structures. Binding site was determined using the prior knowledge of the original ligand interactions site for the respective molecular targets. GoldScore was used as the scoring function to rank the docked compounds.

In the docking simulation studies, each ligand was kept flexible but the amino acid residues of the proteins were held rigid. The selection of atoms in the active site within 10 Å or original ligand was chosen. This protocol was repeated in case of multiple binding sites present in the same protein. The number of best generated pose was set to 10.

### In silico toxicity

L-leucine was subjected to in silico toxicity prediction by analyzing with PROTOX II (Drwal et al. 2014; Erukainure et al. 2018a) and SwissADME (Daina et al. 2017), respectively.

### Statistical analysis

Data were analyzed with one-way analysis of variance (ANOVA) and presented as mean  $\pm$  SD. Significant differences between means were obtained at  $p < 0.05$  using the Tukey's HSD-multiple range post hoc test. Statistical analyses were done using IBM Statistical Package for the Social Sciences (SPSS) for Windows, version 23.0 (IBM Corp., Armonk, NY, USA).

## Results

### In vitro antioxidant and anti-inflammatory activities

As shown in Table 1, in vitro antioxidant analysis revealed L-leucine as a significant ( $p < 0.05$ ) scavenger of free radicals as exhibited by its low  $\text{IC}_{50}$  values of 1.25 and 11.25  $\mu\text{g}/\text{mL}$  for DPPH and ABTS compared to the standard antioxidants.

Additionally, L-leucine significantly ( $p < 0.05$ ) inhibited AChE activity as portrayed by its low  $\text{IC}_{50}$  value of 1.21  $\mu\text{g}/\text{mL}$  (Table 1).

### Ex vivo studies

#### Anti-oxidative activity

Incubation of testicular tissues with  $\text{FeSO}_4$  depleted levels of GSH, SOD and catalase activities, with concomitant elevated level of MDA while depleting the level of non-protein thiol as shown in Fig. 1a–e, indicating an

**Table 1** IC<sub>50</sub> values of biological activities

Activity	(µg/mL)				
	L-leucine	Gallic acid	Galatamine	Ascorbic acid	Quercetin
DPPH	1.25 ± 0.05 <sup>#</sup>	–	–	8.32 ± 0.18	–
ABTS	11.25 ± 0.58 <sup>#</sup>	–	–	–	70.71 ± 2.80
ACHE*	1.21 ± 0.09 <sup>#</sup>	–	48.07 ± 2.9	–	–
GSH	247.35 ± 20.8 <sup>#</sup>	624.57 ± 18.9	–	–	–
SOD	> 1000	128.27 ± 10.11	–	–	–
Catalase	0.19 ± 0.01	0.01 ± 0.001	–	–	–
Lipid Peroxidation	66.40 ± 1.22 <sup>#</sup>	101.22 ± 1.45	–	–	–
Non-Protein Thiol	155.23 ± 3.88	71.94 ± 10.23	–	–	–
ATPase	67.92 ± 2.90 <sup>#</sup>	> 1000	–	–	–
Nitric Oxide	0.01 ± 0.008 <sup>#</sup>	0.38 ± 0.01	–	–	–
Myeloperoxidase	1.77 ± 0.50	0.10 ± 0.09	–	–	–
ACHE <sup>#</sup>	0.01 ± 0.001 <sup>#</sup>	0.70 ± 0.01	–	–	–
Chymotrypsin	7.87 ± 0.50	0.89 ± 0.02	–	–	–
ENTPDase	484.12 ± 12.84 <sup>#</sup>	603.66 ± 20.87	–	–	–
5'NT	> 1000	851.24 ± 20.15	–	–	–

Data = mean; *n* = 3

\*In vitro acetylcholinesterase inhibitory activity

<sup>#</sup>Ex vivo acetylcholinesterase activity, #IC<sub>50</sub> values of L-leucine lower than the standard drugs

occurrence of oxidative damage with a perturbation of the redox balance. Incubation with L-leucine significantly ( $p < 0.05$ ) elevated GSH and non-protein thiol levels, SOD and catalase activities, while depleting the level MDA level. This antioxidant potential is evident by its low IC<sub>50</sub> values as shown in Table 1.

### Proinflammatory activity

As shown in Fig. 2, incubation of testicular tissue with FeSO<sub>4</sub> significantly ( $p < 0.05$ ) elevated NO level and myeloperoxidase activities indicating a proinflammatory activity. These were significantly ( $p < 0.05$ ) prevented on treatment with L-leucine to levels almost indistinguishable from the normal tissues. This is further evident by its low IC<sub>50</sub> values (Table 1).

### Cholinergic and proteolytic activities

Induction of oxidative testicular damage with FeSO<sub>4</sub> significantly ( $p < 0.05$ ) elevated the activities of acetylcholinesterase and chymotrypsin as shown in Fig. 3a and b, respectively. These activities were significantly ( $p < 0.05$ ) reduced dose-dependently on treatment with L-leucine to levels almost indistinguishable from the normal tissues. The low IC<sub>50</sub> values portray a high potency of L-leucine for both activities (Table 1).

### Purinergic enzymes activities

There was a significant ( $p < 0.05$ ) decrease in testicular ATPase, ectonucleotidase (ENTPDase), and 5'nucleotidase (5'NT) activities on induction of oxidative testicular damage with FeSO<sub>4</sub> as shown in Fig. 4a–c, indicating depletion in purinergic enzymatic activities. Treatment of testicular tissues with L-leucine significantly ( $p < 0.05$ ) elevated the activities of these ATP-hydrolysing enzymes to levels almost indistinguishable from the normal tissues. This is further evident by their low IC<sub>50</sub> values compared to the standard drug (gallic acid) (Table 1).

### Testicular metabolites

As shown in Table 2, induction of oxidative testicular damage with FeSO<sub>4</sub> led to depletion of L-lactic acid, nicotinic acid, ascorbic acid-2-sulfate, TG(24:1(15Z)/22:5(4Z,7Z,10Z,13Z,16Z)/o-18:0), ADP, propinol adenylate, and GDP-4-Dehydro-6-deoxy-D-mannose, with concomitant addition of D-4-Hydroxy-2-oxoglutarate, L-cystine, adenosine triphosphate, 6-methylnicotinamide, maleylacetoacetic acid, cholesteryl ester, and 6-Hydroxy flavin adenine dinucleotide compared to the normal tissues. Treatment with L-leucine led to restoration of ascorbic acid-2-sulfate, with concomitant depletion of the oxidative induced metabolites: D-4-Hydroxy-2-oxoglutarate, L-cystine, adenosine triphosphate, maleylacetoacetic acid, cholesteryl ester, and 6-Hydroxy flavin adenine

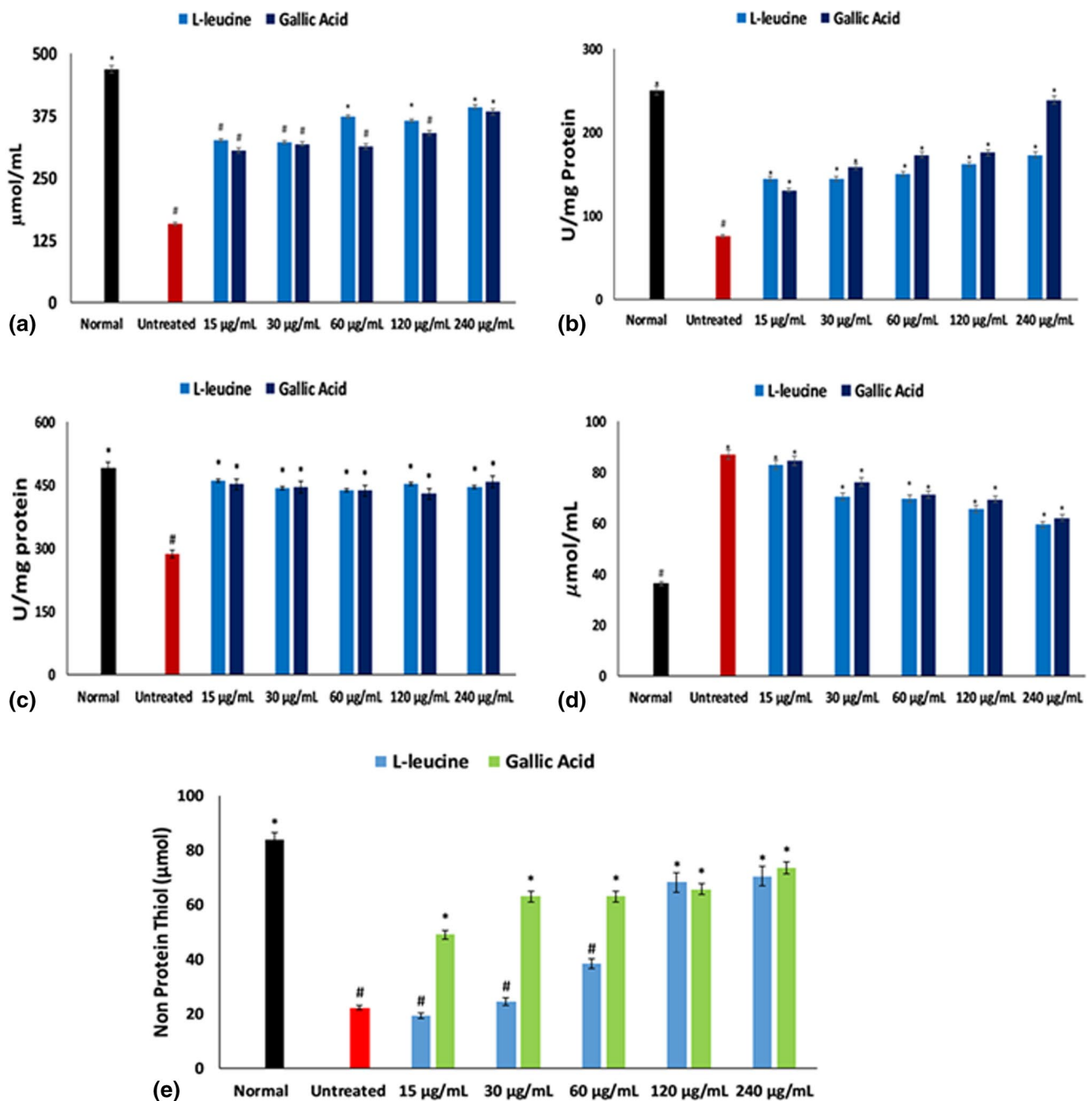


**Fig. 1** Effect of L-leucine on **a** GSH level, **b** SOD activity, **c** catalase activity, **d** MDA level, and **e** non-protein thiol level in oxidative testicular injury. Values = mean  $\pm$  SD;  $n=3$ . \*Significantly different from untreated sample and #Significantly different from normal sam-

ple ( $p < 0.05$ ). Normal: testicular tissue lysates not treated with  $\text{FeSO}_4$  and/or compounds; untreated: testicular tissue lysates treated with  $\text{FeSO}_4$  only

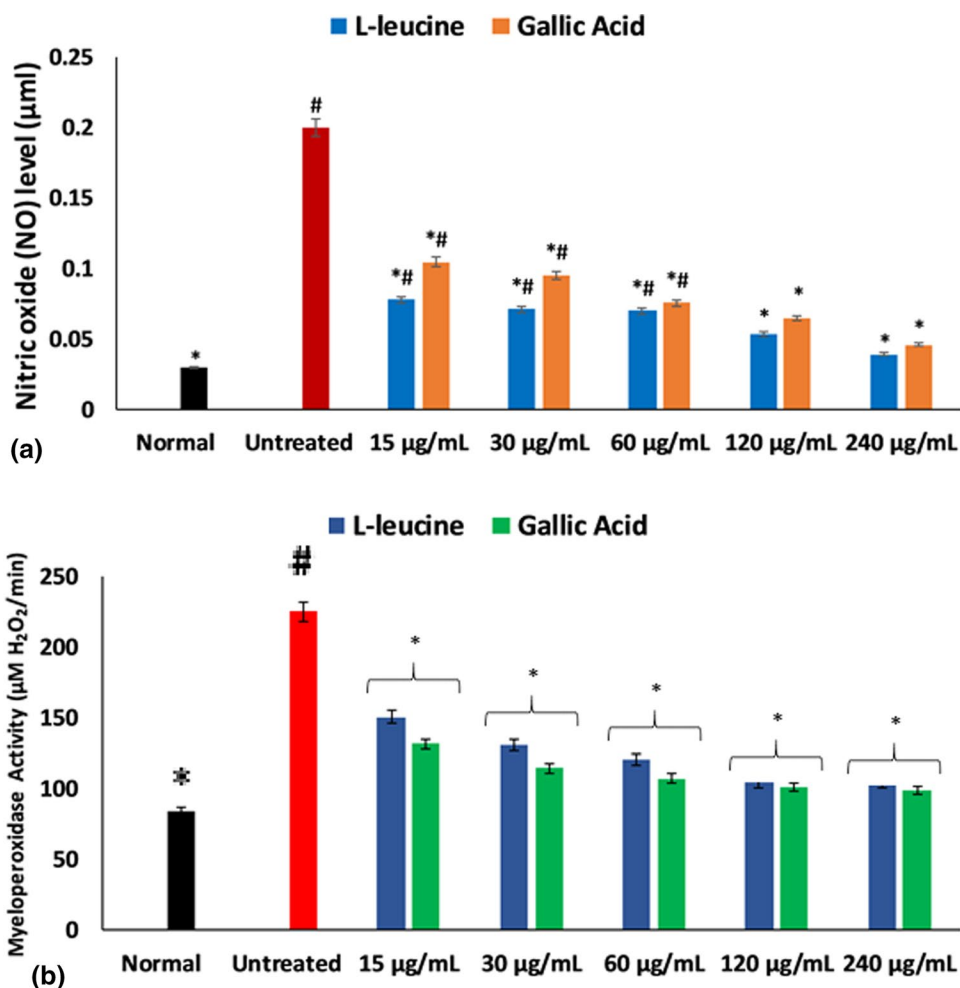
dinucleotide. It also led to the addition of phosphoenolpyruvic acid, IDP, Inositol cyclic phosphate, 2'-deoxyinosine triphosphate, adenosine diphosphate ribose (Table 2).

### Metabolomics

As shown in Fig. 5, pathway analysis of the identified testicular metabolites revealed deactivation of the metabolic



**Fig. 2** Effect of L-leucine on **a** NO level and **b** myeloperoxidase activity in oxidative testicular injury. Values = mean  $\pm$  SD;  $n = 3$ . \*Significantly different from untreated sample and #Significantly different from normal sample ( $p < 0.05$ ). Normal: testicular tissue lysates not treated with  $\text{FeSO}_4$  and/or compounds; untreated: testicular tissue lysates treated with  $\text{FeSO}_4$  only



pathways: propanoate metabolism, fructose and mannose metabolism, pyruvate metabolism, glycolysis, and amino sugar and nucleotide sugar metabolism, while activating the tyrosine metabolism pathway. Treatment with L-leucine led to reactivation of glycolysis while concomitantly deactivating oxidative-induced citrate cycle. Treatment with L-leucine also led to increased significance ( $p < 0.003$ ) of purine metabolism pathway, with an impact fold of  $< 0.001$  (Fig. 5). A schematic pathway network of the identified pathways is presented in Fig. 6.

### DNA protective activity

The effect of L-leucine on  $\text{FeSO}_4$ -induced DNA damage is presented on Fig. 7. In the control lanes (lane 1 and 2) pET151 DNA molecules appears as circular and supercoiled DNA molecules. The addition of  $\text{FeSO}_4$  alone induces the conversion DNA to relaxed linear DNA (lane 3). As expected, Gallic acid protected pET151 DNA the biologically active, open circular DNA from  $\text{FeSO}_4$  induced degradation (lane 4). In the presence of leucine, a dose dependant DNA protective activity was observed. Potent antioxidant

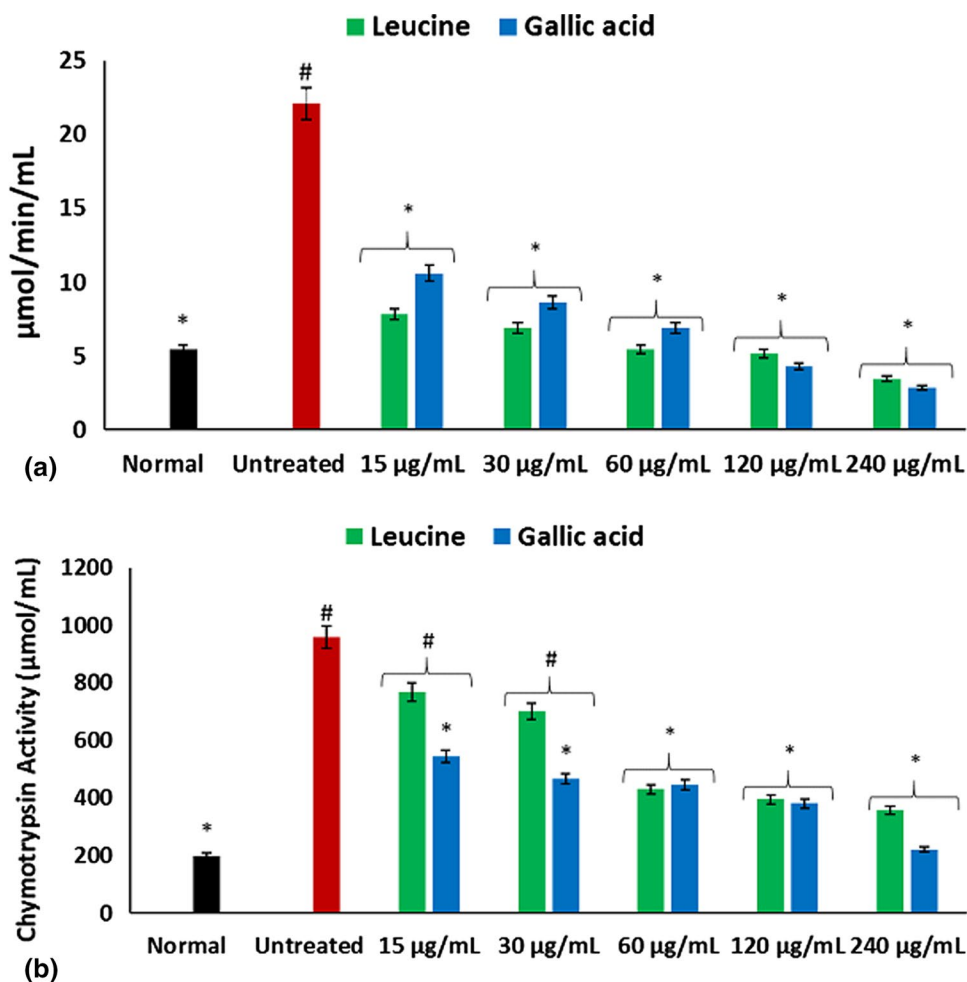
activity by leucine was observed at concentrations of 0.5–5 mg/mL (lanes 7 and 8).

In silico analysis revealed L-leucine binding to the minor groove of the DNA sequence as shown in the different 3D poses (A–C) in Fig. 7b. This is further clarified by the 2D presentation in Fig. 7b (D) which shows minor groove binding forming hydrogen bonds and pi-pi interactions in L-leucine-DNA complex.

### Computational studies

Analyses of the molecular docking poses indicated L-leucine as potent inhibitors of COX-2, IL-1 beta and iNOS (Figs. 8, 9, 10). Computational docking of L-leucine to COX-2 (PDB code: 5F19) suggest that L-leucine binds in the same cavity as the original ligand (B-octylglucoside). The ligand-receptor interaction diagram revealed L-leucine interacts with the residues ARG-185, ARG-438, and GLU-490 of the B chain of the receptor (Fig. 8a and b). Additionally, docking with the receptor IL-1 (beta) having PDB code: 4GAF, L-leucine interacts with the residues ARG-272 and THR-234 of B chain, similarly as the interaction present with original

**Fig. 3** Effect of L-leucine on **a** acetylcholinesterase and **b**  $\alpha$ -chymotrypsin activities in oxidative testicular injury. Values = mean  $\pm$  SD;  $n = 3$ . \*Significantly different from untreated sample and #Significantly different from normal sample ( $p < 0.05$ ). Normal: testicular tissue lysates not treated with  $\text{FeSO}_4$  and/or compounds; untreated: testicular tissue lysates treated with  $\text{FeSO}_4$  only



ligand (N-acetyl-D-glucosamine) (Fig. 9a and b). Results obtained from the iNOS (PDB code: 1NSI)-Leucine docking study suggests: L-leucine interacts with the residues ILE-462 and ARG-381 of the chain A; similar interactions are also observed between the receptor and its original ligand (5,6,7,8- tetrahydrobiopterin) (Fig. 10a and b).

### Cytotoxicity

Cytotoxicity analysis of L-leucine against HFF cell lines showed that the amino acid is not cytotoxic against the cell lines as shown in Fig. 11, with an  $\text{IC}_{50}$  value of  $\geq 50$  mg/mL. The standard drug, staurosporine however displayed a cytotoxic effect against the cell lines.

### In silico toxicology

Meanwhile, analysis by in silico toxicology predicted the oral toxicity  $\text{LD}_{50}$  of L-leucine to be 5000 mg/kg, with a toxicity class value of 5 (Table 3). The amino acid was predicted not to be a substrate for P-glycoprotein, CYP2D6 and

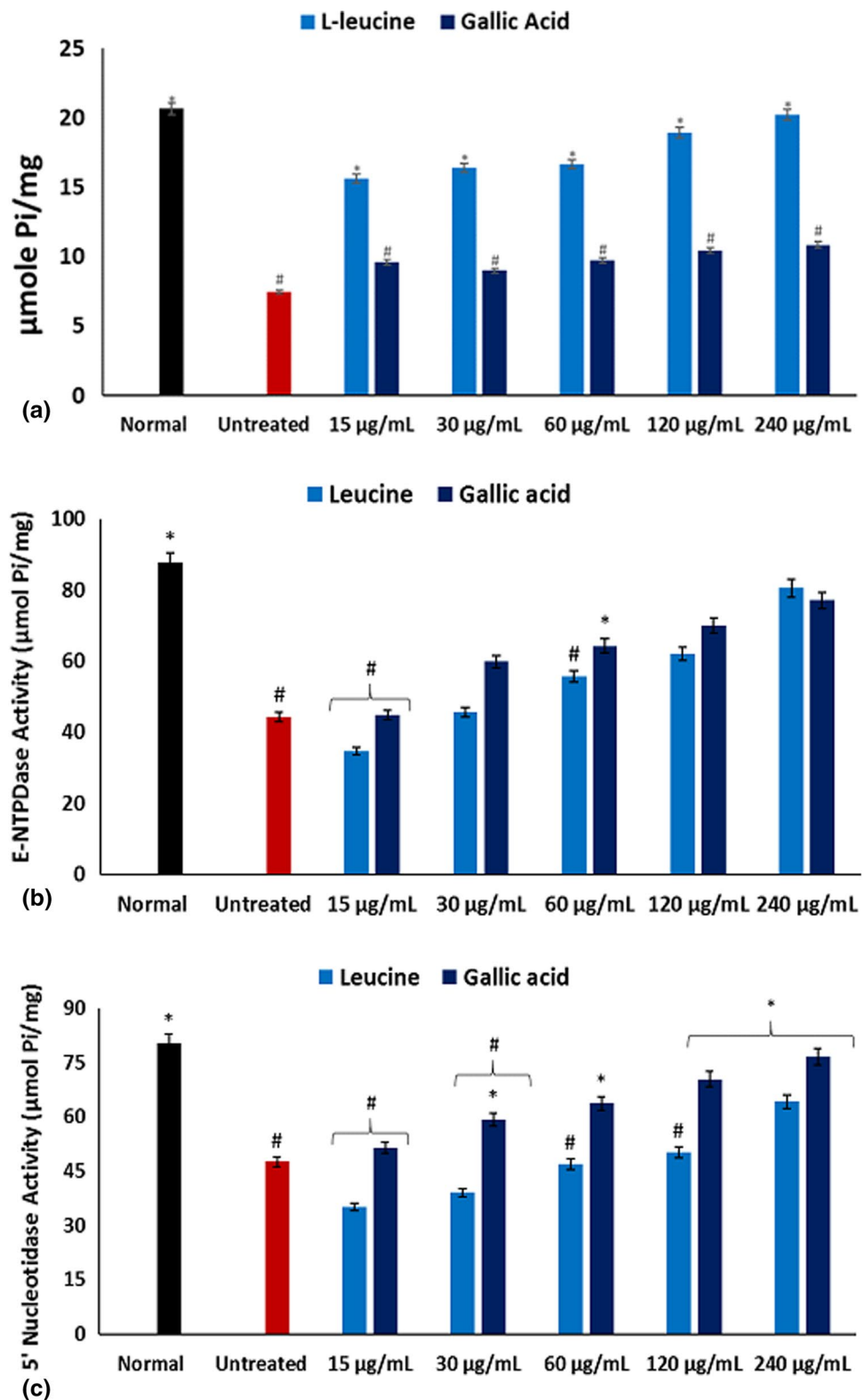
CYP3A4. L-leucine was also predicted not to be an inhibitor of CYP1A2, CYP2C19, CYP2C9, CYP2D6, and CYP3A4.

## Discussion

Testicular toxicity leading to male infertility in the long run is a major health issue particularly in developing countries where children are considered blessings among married couples. Several factors have been recognized as major contributors of testicular toxicity, with oxidative injury being reported among the patho-mechanism. In the present study, we investigated the protective effect of L-leucine on oxidative-mediated testicular injury using in vitro, ex vivo and in silico models.

The therapeutic properties of branched chain amino acids (BCAAs) has been reported. They have been reported for their ability to modulate glucose homeostasis, maintain muscle integrity (Cojocaru et al. 2014; Ham et al. 2014; Nicastro et al. 2012). In this study, the therapeutic effect of the BCAA, L-leucine was investigated on oxidative testicular injury.

**Fig. 4** Effect of L-leucine on **a** ATPase, **b** ENTPDase, and **c** 5' nucleotidase activities in oxidative testicular injury. Values = mean  $\pm$  SD;  $n = 3$ . \*Significantly different from untreated sample and #Significantly different from normal sample ( $p < 0.05$ ). Normal: testicular tissue lysates not treated with  $\text{FeSO}_4$  and/or compounds; untreated: testicular tissue lysates treated with  $\text{FeSO}_4$  only



Oxidative stress has been implicated in the dysfunction of the male reproductive system, which has been attributed to the high susceptibility of the testicular polyunsaturated fatty acids (PUFAs) to free radical attack (Erukainure

et al. 2019b; Obode et al. 2015). The depleted GSH and non-protein thiol levels, SOD and catalase activities in the untreated tissues (Fig. 1) indicates oxidative injury and can be attributed to the generation of free radicals by  $\text{Fe}^{2+}$  via

**Table 2** LC–MS identified metabolites of testicular tissues

Metabolites	Normal tissue	Untreated tissue	Treated tissue
3-Mercaptolactic acid	X	X	X
3-Mercaptopyruvic acid	X	X	X
L-Cysteinylglycine disulfide	X	X	–
L-Lactic acid	X	–	–
Dimethylallylpyrophosphate	X	X	–
Nicotinic acid	X	–	–
Succinic acid	X	X	X
Ascorbic acid-2-sulfate	X	–	X
TG(24:1(15Z)/22:5(4Z,7Z,10Z,13Z,16Z)/o-18:0)	X	–	–
ADP	X	–	–
Propinol adenylate	X	–	–
GDP-4-Dehydro-6-deoxy-D-mannose	X	–	–
D-4-Hydroxy-2-oxoglutarate	–	X	–
L-Cystine	–	X	–
Adenosine triphosphate	–	X	–
6-Methylnicotinamide	–	X	X
Maleylacetoacetic acid	–	X	–
cholesteryl ester	–	X	–
6-Hydroxy flavin adenine dinucleotide	–	X	–
Phosphoenolpyruvic acid	–	–	X
IDP	–	–	X
Inositol cyclic phosphate	–	–	X
2'-Deoxyinosine triphosphate	–	–	X
Adenosine diphosphate ribose	–	–	X

X present, – not present. Normal tissue: testicular tissues not incubated with FeSO<sub>4</sub> or L-leucine; untreated tissue: testicular tissues incubated with FeSO<sub>4</sub> only; treated tissues: testicular tissues incubated with FeSO<sub>4</sub> and L-leucine

the Fenton reaction (Aslan et al. 2000) Superoxide, O<sub>2</sub><sup>•−</sup> has been recognized as the main free radical produced by the spermatozoa (Hsieh et al. 2002) which explains the high testicular level of SOD (Aitken and Roman 2008; Mruk et al. 2002). Alteration of the normal testicular physiology often results to increased production of O<sub>2</sub><sup>•−</sup> which overwhelms the SOD activity, and undergoes putative protonation to yield the perhydroxyl radical (·OOH) (Kanas and Acker 2010). The generated hydrogen peroxide, H<sub>2</sub>O<sub>2</sub> from the dismutation of O<sub>2</sub><sup>•−</sup> by SOD if not broken down by catalase, will generate hydroxyl radical (•OH). Both •OH and ·OOH have been implicated in the peroxidation of the membrane lipids. This is evident in the present study by the high MDA level in the untreated tissue (Fig. 1d). The elevated levels of GSH, non-protein thiol, SOD and catalase activities, with concomitant depletion of MDA level in the treated testicular tissues (Fig. 1a–e) therefore indicates an antioxidative effect of L-leucine in oxidative testicular injury. This is further evident by the high free radical scavenging activities of L-leucine (Table 1).

Proinflammation has also been linked with the progression of oxidative testicular toxicity, with the generation of

reactive oxygen species (ROS) recognized as a major mechanistic link (Azenabor et al. 2015; Nicastro et al. 2012). The increased generated O<sub>2</sub><sup>•−</sup> can react with NO, leading to the production of peroxynitrite (ONOO<sup>−</sup>), a potent free radical (Erukainure et al. 2018b). Hydroxyl radicals generated from the breakdown of H<sub>2</sub>O<sub>2</sub> can also react with hydrochloric acid (HCl) in the presence of myeloperoxidase to generate hypochlorous acid (HOCl<sup>−</sup>) (Erukainure et al. 2018b; Furtmüller et al. 2000). Thus, the elevated level of NO and myeloperoxidase activity in the untreated tissue (Fig. 2a and b) demonstrates a proinflammatory effect. The depleted NO level and myeloperoxidase activity in the treated tissues, therefore indicates an anti-proinflammatory effect of L-leucine in oxidative testicular injury. This is further evident by the molecular interactions of L-leucine with the inflammatory cytokine, IL-β, and the cytokine-inducible cyclooxygenase (COX-2) and nitric oxide synthases (iNOS) (Figs. 8, 9, 10). Although these cytokines play major roles in the regulation of spermatogenesis and steroidogenesis in normal testes, their detrimental roles have however been reported in the progression of inflammation (Guazzone et al. 2009). The anti-inflammatory effect of L-leucine was also demonstrated

by its ability to inhibit AChE activity in vitro (Table 1) as inhibition of the enzyme activity has been linked with anti-inflammatory effects in several studies (Chougouo et al. 2016; Osunsanmi et al. 2019). These results correspond with previous reports on the anti-inflammatory effect of L-leucine (Ham et al. 2014; Nicastro et al. 2012).

Up regulation of testicular acetylcholinesterase activity has been linked to impaired testicular function which can contribute to male infertility (Andersson 2003, 2011). The exacerbated acetylcholinesterase activity on induction of oxidative testicular injury (Fig. 3a) reflects an alteration in acetylcholine level, which portrays an impaired testicular function. The increased activity may be attributed to the induction of oxidative stress (Fig. 1). Oxidative stress has been implicated in the exacerbation of acetylcholinesterase activity (Melo et al. 2003). Inhibition of acetylcholinesterase activity has been employed in the treatment and management of testicular toxicity (Akamolafe et al. 2017; Andersson 2011). Thus, the suppressed activity in tissues treated with L-leucine suggests an improved testicular function which corroborates with the exacerbated testicular antioxidant activity (Fig. 1).

The role of proteolysis in the complex process of tissue maintenance, repair, growth and development have been reported (Le Magueresse-Battistoni 2007). An alteration in this activity has been implicated in the pathogenesis and progression of several pathological processes such as cancer, infertility, cardiovascular diseases, and neurodegeneration (Le Magueresse-Battistoni 2007). In the present study, the increased  $\alpha$ -chymotrypsin activity in the untreated testicular tissues indicates an elevated proteolysis on induction of oxidative stress (Fig. 3b).  $\alpha$ -chymotrypsin is a proteolytic enzyme that degrades proteins and polypeptides (Panner Selvam et al. 2018). Thus, the decreased activity in the treated testicular tissues portrays an anti-proteolytic effect of L-leucine.

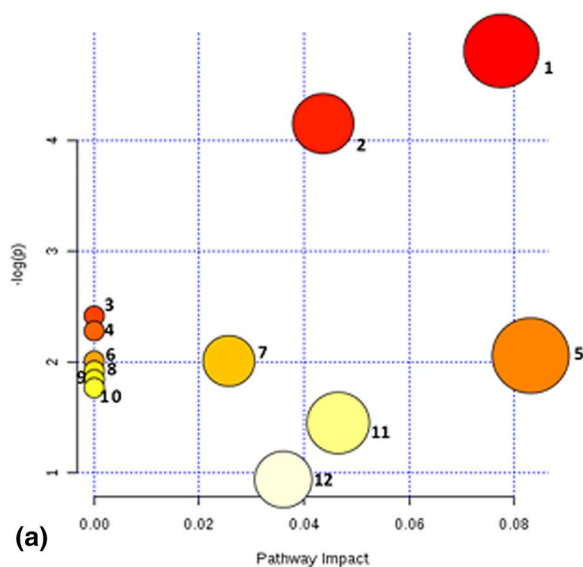
The suppressed purinergic activities in untreated testicular tissues as shown by the decreased ATPase (Fig. 4a), ENTPDase (Fig. 4b), and 5'NT (Fig. 4c) activities suggests an alteration in testicular nucleotide metabolism on induction of oxidative damage. These enzymes have been reported to play major roles in testicular functions and fertility (Burnstock 2014; Gorodeski 2015). The purinergic alterations in the untreated tissues further indicate a testicular dysfunction on induction of oxidative damage. The exacerbated activities of these enzymes in the treated tissues (Fig. 4a–c) suggests the ability of L-leucine to upregulate the nucleotide hydrolysis in oxidative testicular injury.

The induced oxidative damage in the untreated testicular tissues corresponds with the depleted antioxidant

metabolites, nicotinic acid and ascorbic acid-2-sulfate (Table 2). The presence of the gamma keto-acid metabolite, D-4-Hydroxy-2-oxoglutarate may be attributed to generation of ATP for sperm motility (Li et al. 2010). The presence of L-cysteine portrays generation of L-cysteine thiyl radical from metallic oxidation of L-cysteine (Harman et al. 1984). The ATP metabolite portrays an increased mitochondrial respiration, insinuating generation of  $O_2^{\bullet-}$  which establishes a proton gradient within the mitochondria (Velarde 2014). Owing to the low antioxidant enzyme activity of the untreated tissue (Fig. 1a–c), the continuous generation of  $O_2^{\bullet-}$  could lead to oxidative stress.

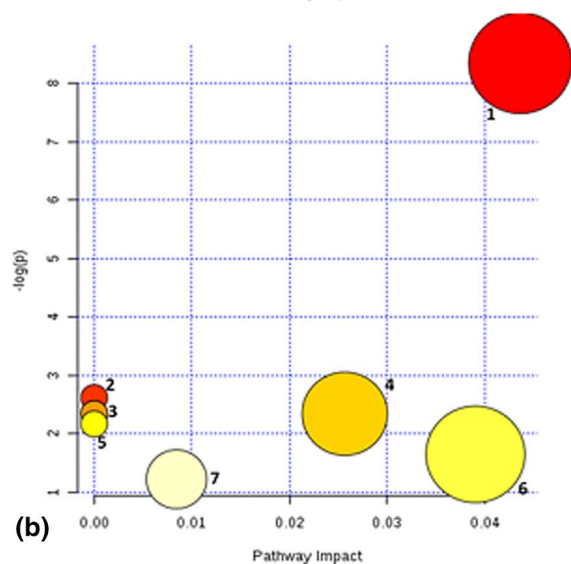
Activation of tyrosine metabolism in the untreated tissue (Figs. 5 and 6) corroborates the maleylacetoacetic acid metabolite in the tissue (Table 2). Maleylacetoacetic acid is a metabolite of tyrosine degradation (Lantum et al. 2003). Activation of this pathway as well as elevated levels of NO (Fig. 2a) may insinuate tyrosine nitration. Continuous nitration of tyrosine has been linked with elevated reactive nitrogen species (RNS) levels thus contributing to inflammatory process (Koeck et al. 2005). The presence of Krebs cycle with concomitant depleted L-lactic acid in the untreated tissues may indicate a switch from ATP production from anaerobic glycolysis to oxidative phosphorylation via the generation of electron donors, NADH and FADH<sub>2</sub>. Studies have implicated decreased glycolytic phosphorylation and concomitant elevated oxidative phosphorylation in impaired sperm motility (Tourmente et al. 2015). The activation of pyruvate metabolism and glycolysis with concomitant inactivation of Krebs cycle in testicular tissues treated with L-leucine indicates a switch to glycolytic phosphorylation from oxidative phosphorylation, which is of importance to sperm motility. Accumulation of NADH and FADH<sub>2</sub> generated from Krebs cycle has been linked to the production of ROS via the electron transport chain, thereby leading to oxidative stress (Brownlee 2001; Du et al. 2001). Deactivation of these pathways in the treated testicular tissues further portrays the therapeutic effect of L-leucine on oxidative testicular injury.

Spermatic DNA fragmentation has been recognized as one of the main hallmarks of male infertility (Agarwal et al. 2017). It is often caused by oxidative stress during spermatogenesis, epididymal storage, and ejaculation (Homa et al. 2019). In the present study, the protective effect of L-leucine on oxidative DNA fragmentation was investigated in plasmid DNA. The ability of L-leucine to maintain the original super circular form of the DNA (Fig. 7), therefore indicates the potential of the amino acid to protect and maintain the morphology of DNAs exposed to oxidative stress. This is further portrayed by its molecular interaction with DNA in silico (Fig. 7b).



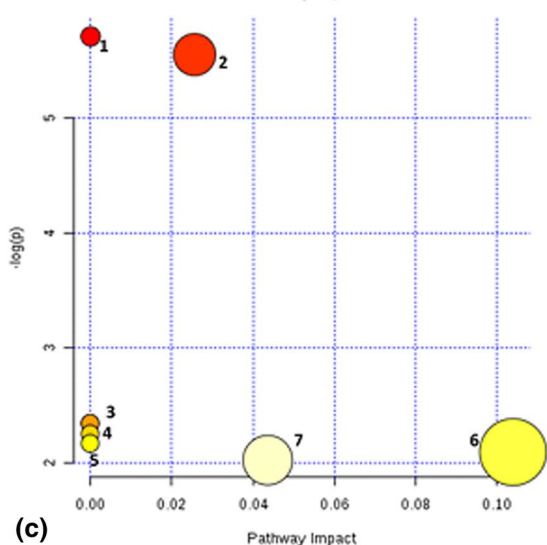
### Legend

1. Propanoate metabolism
2. Cysteine and methionine metabolism
3. Nicotinate and nicotinamide metabolism
4. Terpenoid backbone biosynthesis
5. Fructose and mannose metabolism
6. Butanoate metabolism
7. Citrate cycle (TCA cycle)
8. Pyruvate metabolism
9. Alanine, aspartate and glutamate metabolism
10. Glycolysis
11. Amino sugar and nucleotide sugar metabolism
12. Purine metabolism



### Legend

1. Cysteine and methionine metabolism
2. Terpenoid backbone biosynthesis
3. Butanoate metabolism
4. Citrate cycle (TCA cycle)
5. Alanine, aspartate and glutamate metabolism
6. Tyrosine metabolism
7. Purine metabolism



### Legend

1. Purine metabolism
2. Citrate cycle (TCA cycle)
3. Butanoate metabolism
4. Pyruvate metabolism
5. Alanine, aspartate and glutamate metabolism
6. Glycolysis
7. Cysteine and methionine metabolism

**Fig. 5** Pathway analysis of the most relevant metabolic pathways in **a** normal testicular tissues, **b** untreated testicular tissues, and **c** L-leucine-treated testicular tissues. Normal: testicular tissue lysates not treated with FeSO<sub>4</sub> and/or compounds; untreated: testicular tissue lysates treated with FeSO<sub>4</sub> only

There are increasing concerns on the safety and toxicity of natural products, with questions on their standardization, characterization and preparation (Ezuruike and Prieto 2014). The predicted toxicity class and LD<sub>50</sub> value of L-leucine (Table 3) portrays the safety of the amino acid if orally consumed. The predicted inability of L-leucine to inhibit CYPs 1A2, 2C19, 2C9, 2D6, and 3A4 (Table 3) suggests a non-toxic effect when the amino acid is co-administered with other food and/or drug products that are metabolized

by these enzymes. The little or no cytotoxic effect of L-leucine on HFF (Fig. 11) further demonstrates the safety of the amino acid on normal mammalian cells.

In conclusion, the experimental as well as computational investigations suggest a wide range of applications of L-leucine as a therapy against oxidative testicular injury. These results indicate the therapeutic and protective potentials of L-leucine on oxidative testicular injury, as evident by its ability to attenuate oxidative stress and proinflammation, while stalling cholinergic dysfunction and modulating nucleotide hydrolysis; as well as modulate oxidative dysregulated metabolites and their pathways. L-leucine may thus serve as a dietary supplement and/or nutraceutical in the treatment and management of testicular dysfunction. However, in vivo studies are recommended to further validate these claims.

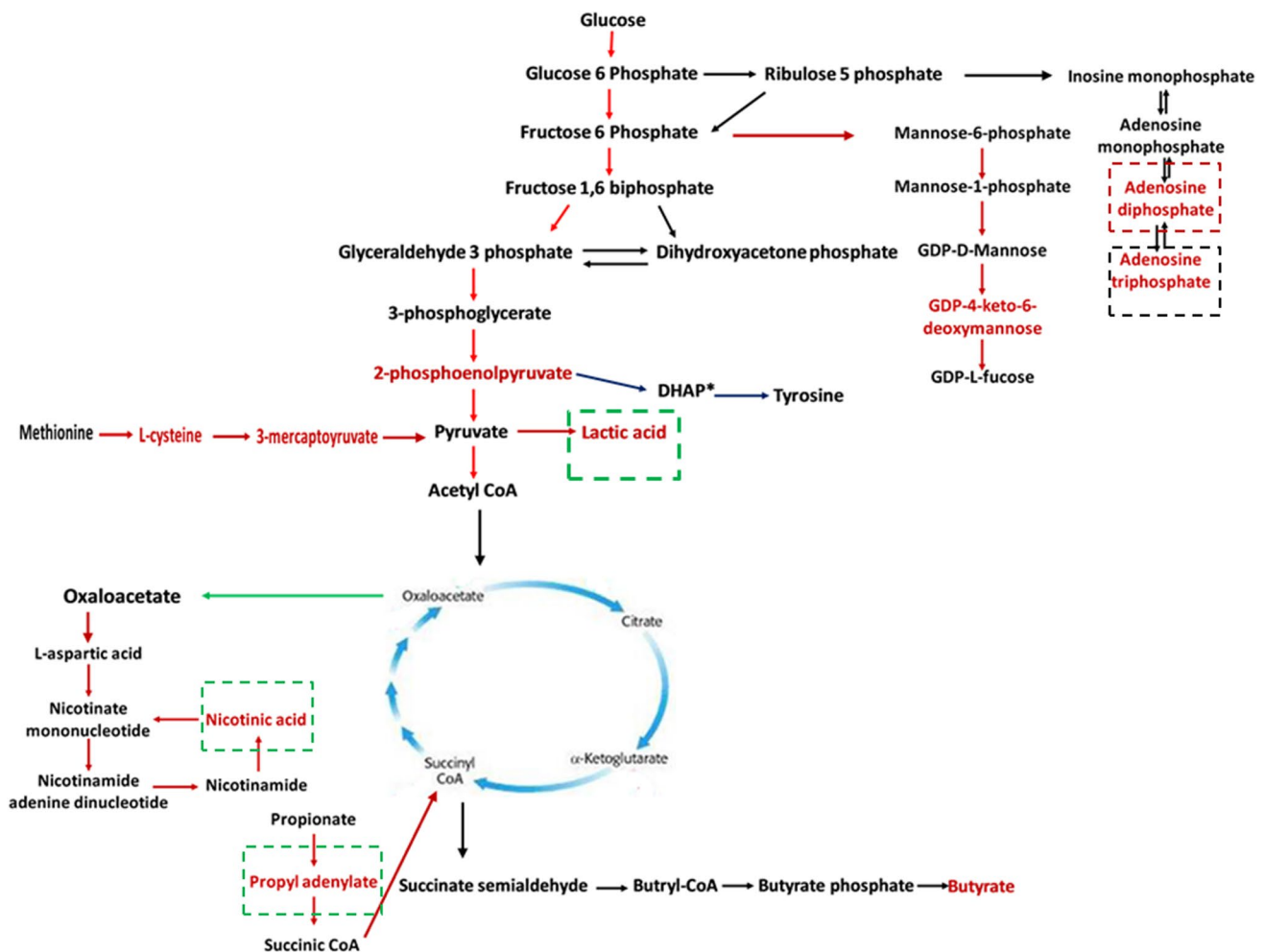
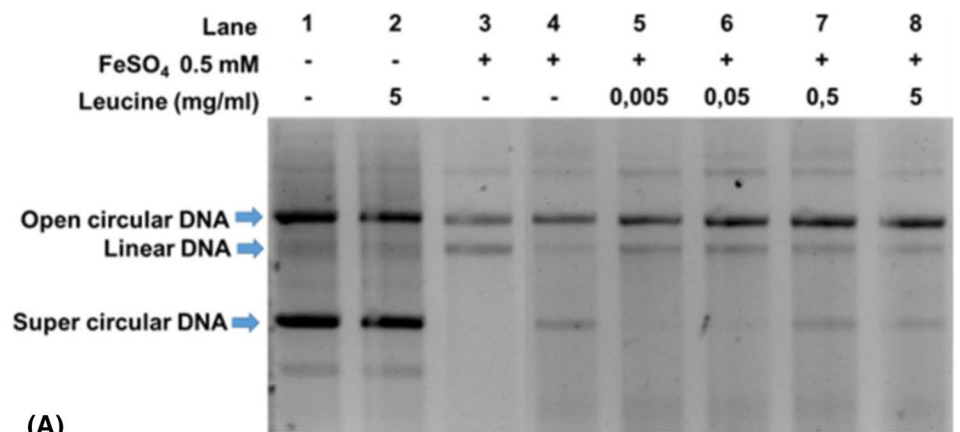


**Fig. 6** Schematic network of the most relevant metabolic pathways in the studied testicular tissues. Metabolites in red colors are identified metabolites. Red and blue arrows represent pathways in normal and untreated testicular tissues, respectively, while black arrows represent pathways common to all tissues. Black dash boxes: generated metab-

olites in untreated testicular tissues; red dash boxes: generated metabolite in treated testicular tissues; green dash boxes: altered metabolites in untreated and treated testicular tissues. Normal: testicular tissue lysates not treated with FeSO<sub>4</sub> and/or compounds; untreated: testicular tissue lysates treated with FeSO<sub>4</sub> only

**Fig. 7 a** DNA protective role of leucine on  $\text{FeSO}_4$  induced DNA oxidative damage. Lane 1 and 2 represent the native DNA and DNA treated with 5000  $\mu\text{g}/\text{mL}$  of leucine; Lane 3 represents plasmid DNA treated  $\text{FeSO}_4$ . Lane 4 represent challenged  $\text{FeSO}_4$  in the presence of a commercial antioxidant Gallic acid (1  $\text{mg}/\text{mL}$ ). Lanes 5–8, represent the DNA challenged  $\text{FeSO}_4$  in the presence of increasing concentration of leucine (0,005–5  $\text{mg}/\text{mL}$ , respectively). **b** Computational prediction of molecular interaction between of L-leucine and DNA



(A)

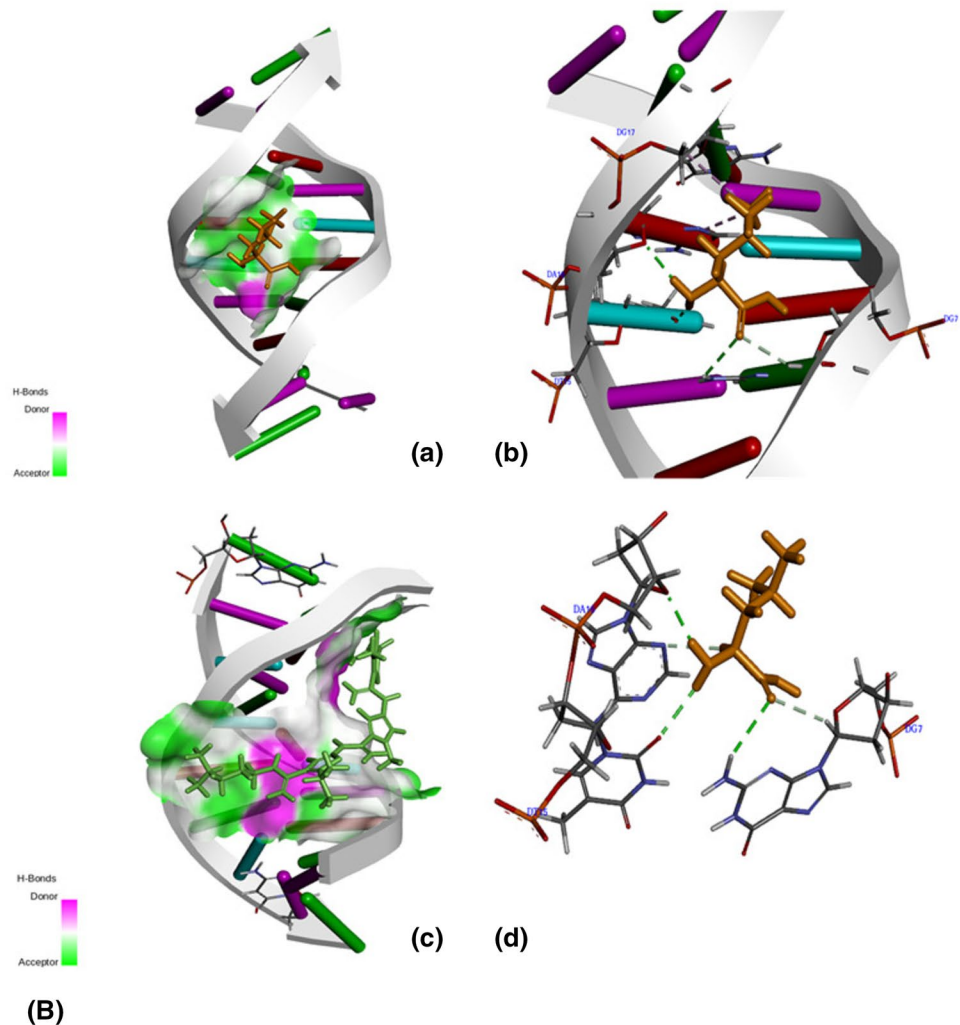




**Fig. 8 a** Computational prediction of binding mode of leucine-COX-2 (left) original ligand in pink and (right) L-leucine in orange docked into the crystal structure of the COX-2 protein (blue). The interactive protein residues are highlighted in green. **b** Interaction between receptor side chains and docked ligand: (Left) binding mode interactions of the original ligand with the receptor (PDB code: 5F19), the ligand interacts with the residues ARG185, ARG438, GLU490 of the chain B. Similarly (right) L-leucine interacts with the residues ARG438, ARG185, GLU490 of the chain B

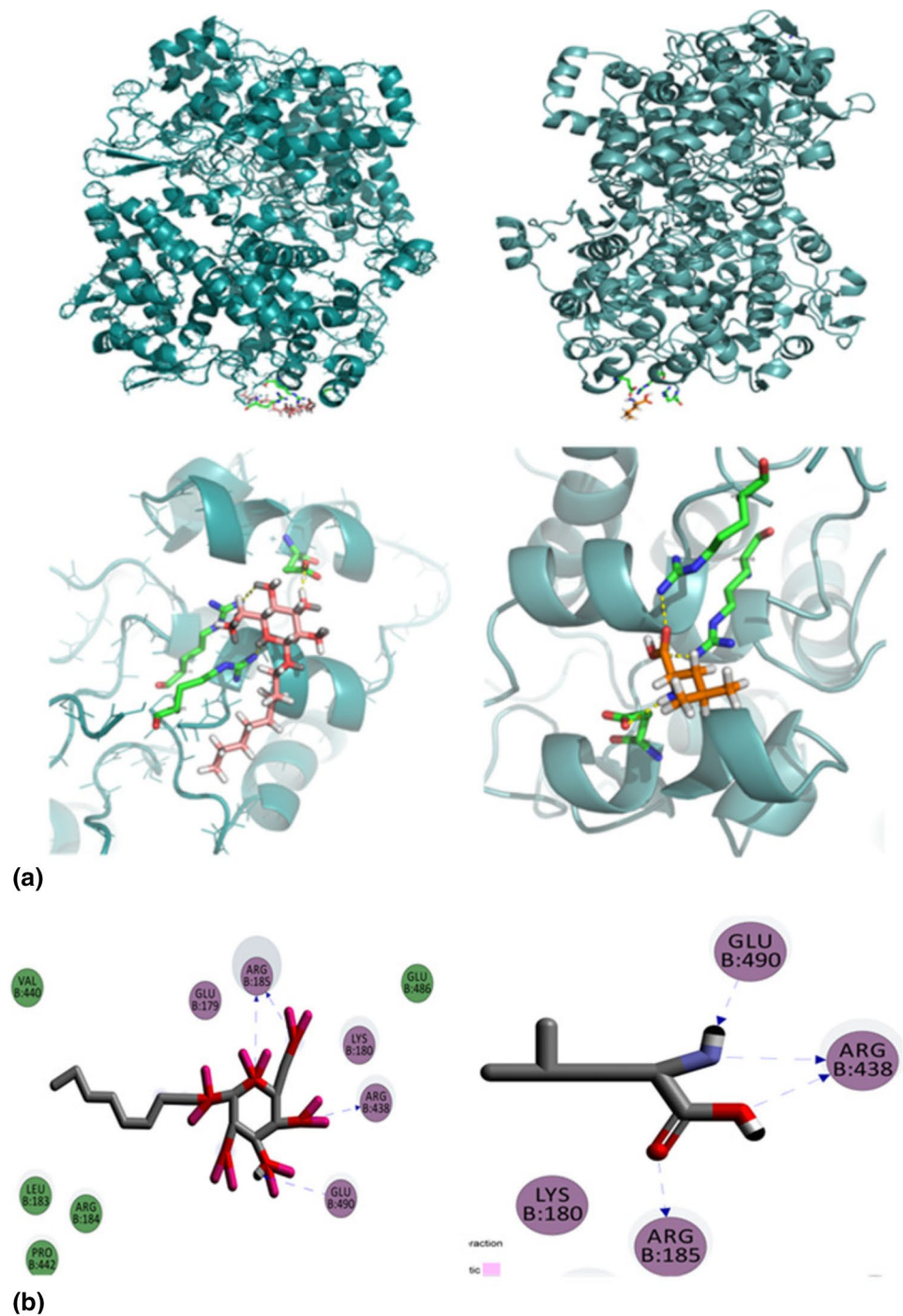


**Fig. 9** **a** Computational prediction of binding mode of leucine- IL-1 beta (left) original ligand in pink and (right) L-leucine in orange docked into the crystal structure of the IL-1 beta protein (brown). The interactive protein residues are highlighted in green. **b** Interaction between receptor side chains and docked ligand: (Left) binding mode interactions of the original ligand with the receptor (PDB code: 4GAF), the ligand interacts with the residues ARG272, THR234, VAL212 of the chain B. Similarly (right) L-leucine interacts with the residues ARG272, THR234 of the chain B

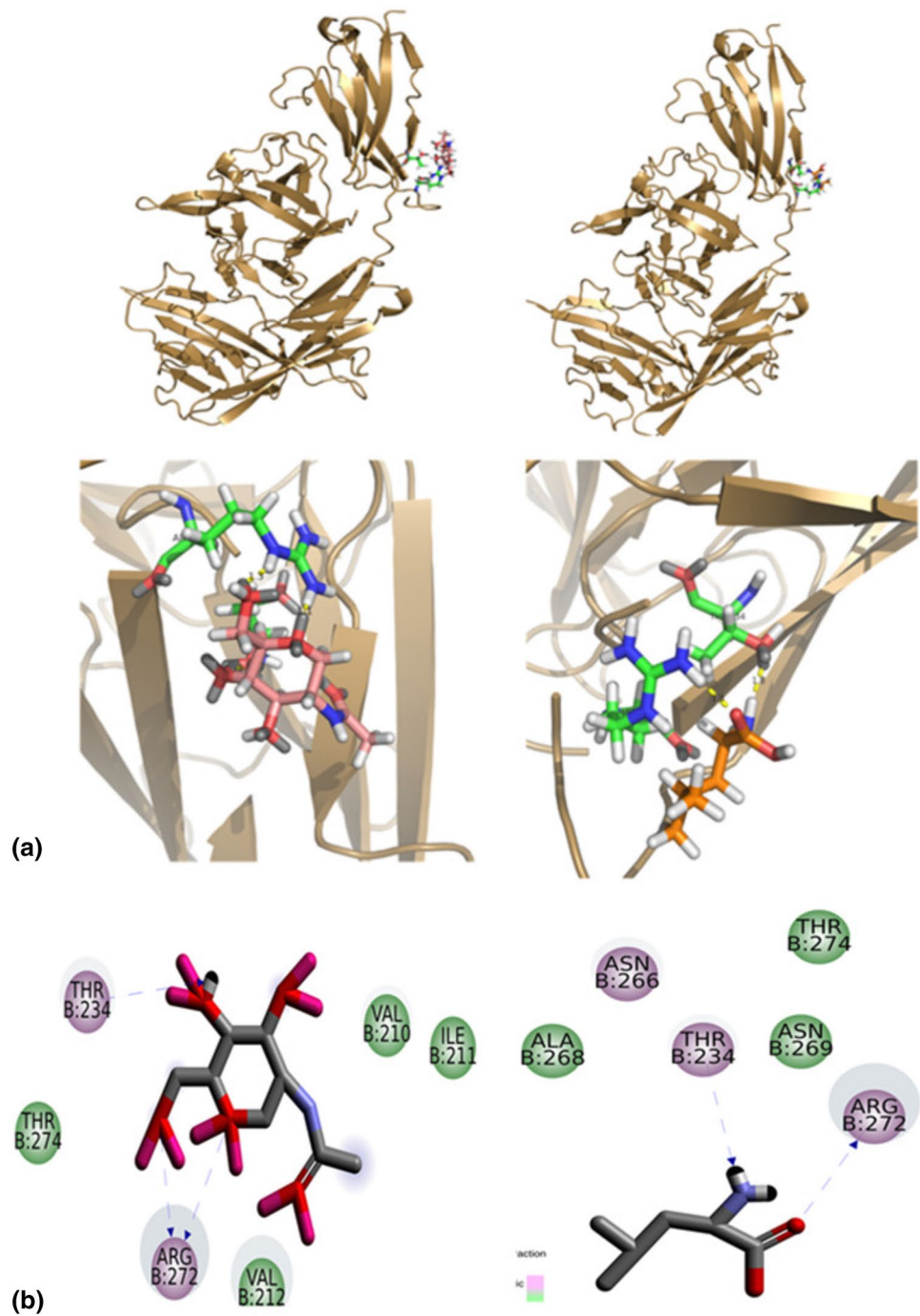


**Fig. 10 a** Computational prediction of binding mode of leucine-iNOS (left) original ligand in blue and (right) L-leucine in orange docked into the crystal structure of the iNOS protein (red). The interactive protein residues are highlighted in green. **b** Interaction between receptor side chains and docked ligand: (Left) binding mode interactions of the original ligand with the receptor (PDB code: 1NSI), the ligand interacts with the residues ILE462, SER118, TRP463 of chain A and PHE476, of the chain B. (right) L-leucine interacts with the residues ILE 462 and ARG 381 of the chain A

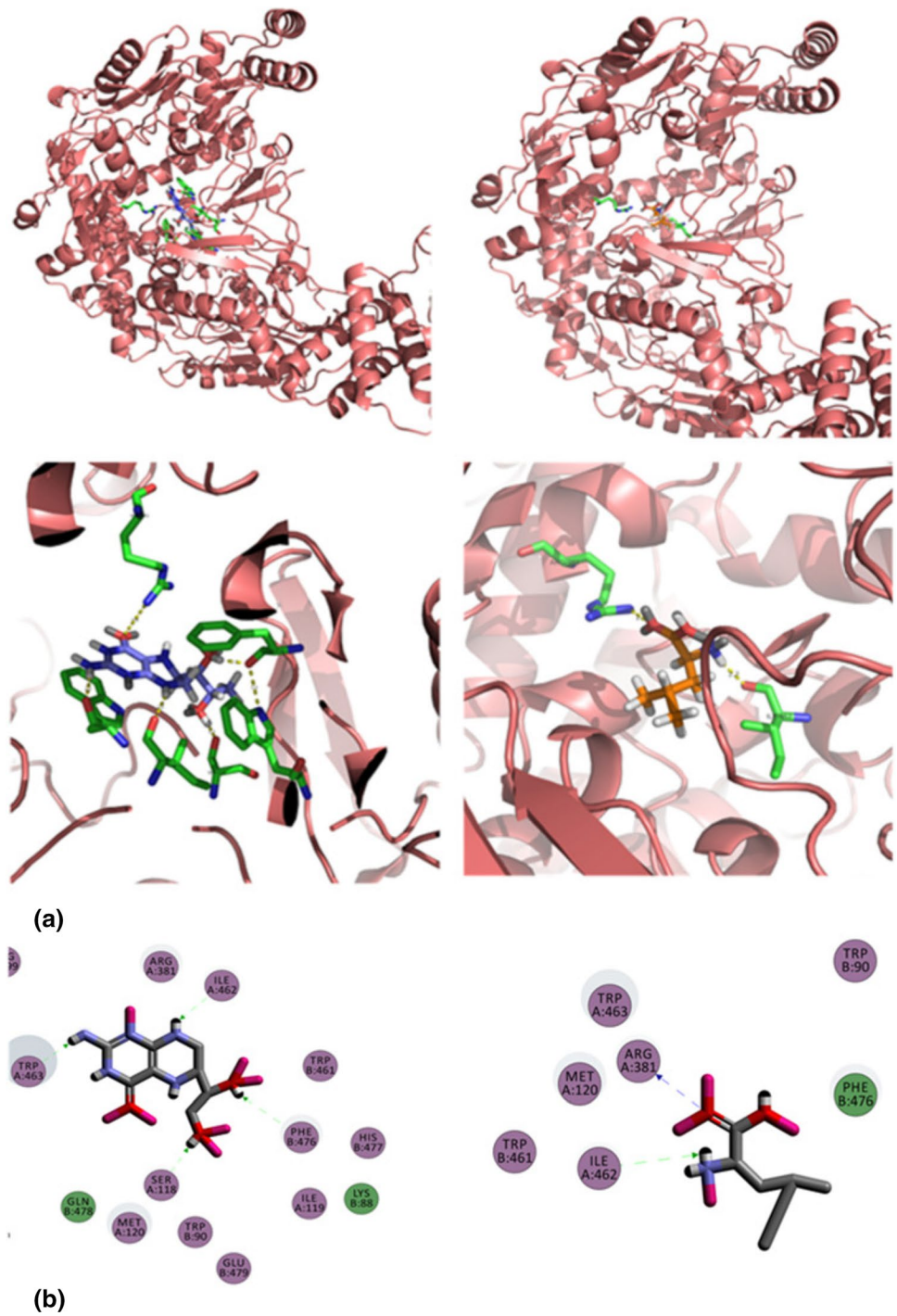


**Fig. 11** Cytotoxic effect of L-leucine on HFF cells. Values = mean  $\pm$  SD;  $n = 3$

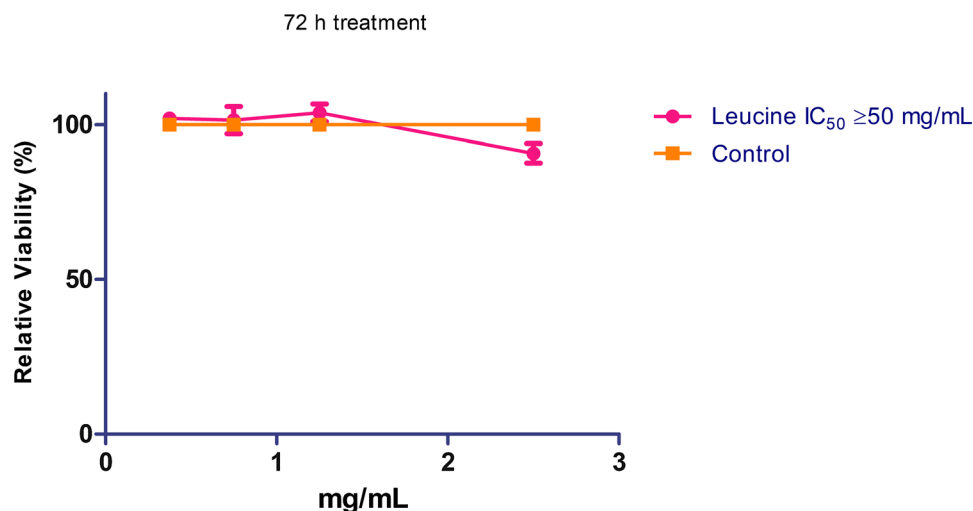


**Table 3** Predicted in silico toxicity of L-leucine

Parameters	Predicted values
Gastrointestinal absorption	High
P-glycoprotein substrate	No
CYP2D6 substrate	No
CYP3A4 substrate	No
CYP1A2 Inhibitor	No
CYP2C19 Inhibitor	No
CYP2C9 Inhibitor	No
CYP2D6 Inhibitor	No
CYP3A4 Inhibitor	No
Oral toxicity LD <sub>50</sub> (rats)	5000 mg/kg
Toxicity Class	5

**Acknowledgement** There was no financial assistance for this study

**Author contributions** Biological activities: OE, OA, OSA, OJP, CIC, and SI; LCMS analysis: OE, SI, and NK; computational Studies: PB, RA and RP; writing-original draft preparation: OE, OA, and PB; writing-review and editing: all authors.

### Compliance with ethical standards

**Conflict of interest** The authors declare that they have no conflict of interest.

**Research involving human participants and/or animals** Ethical approval for the present study was obtained from the Animal Ethics Committee of the University of KwaZulu-Natal, Durban, South Africa (Protocol approval number: AREC/020/017D).

### References

- Abd-Allah AR, Helal GK, Al-Yahya AA, Aleisa AM, Al-Rejaie SS, Al-Bakheet SA (2009) Pro-inflammatory and oxidative stress pathways which compromise sperm motility and survival may be altered by L-carnitine. *Oxid Med Cell Longev* 2(2):73–81
- Adefegha SA, Rosa Leal DB, Olabiyi AA, Oboh G, Castilhos LG (2017) Hesperidin attenuates inflammation and oxidative damage in pleural exudates and liver of rat model of pleurisy. *Redox Rep* 22(6):563–571
- Ademiluyi AO, Ogunsuyi OB, Oboh G (2016) Alkaloid extracts from Jimson weed (*Datura stramonium* L.) modulate purinergic enzymes in rat brain. *Neurotoxicology* 56:107–117
- Adewoye O, Bolarinwa A, Olorunsogo O (2000) Ca<sup>++</sup>, Mg<sup>++</sup>-ATPase activity in insulin-dependent and non-insulin dependent diabetic Nigerians. *Afri J Med Med Sci* 29(3–4):195–199
- Aebi H (1984) Catalase in vitro. *Method Enzymol* 105:121–126
- Agarwal A, Cho C-L, Esteves SC, Majzoub A (2017) Reactive oxygen species and sperm DNA fragmentation. *Transl Androl Urol* 6(Suppl 4):S695
- Aitken RJ, Roman SD (2008) Antioxidant systems and oxidative stress in the testes. *Oxid Med Cell Longev* 1(1):15–24
- Akinyemi AJ, Onyebueke N, Faboya OA, Onikanni SA, Fadaka A, Olayide I (2017) Curcumin inhibits adenosine deaminase and arginase activities in cadmium-induced renal toxicity in rat kidney. *J Food Drug Anal* 25(2):438–446
- Akomolafe S, Oboh G, Olasehinde T, Oyeleye S, Ogunsuyi O (2017) Modulatory effects of Aqueous extract from *Tetracarpidium conophorum* leaves on key enzymes linked to erectile dysfunction and oxidative stress-induced lipid peroxidation in penile and testicular tissues. *J Appl Pharm Sci* 7(01):051–056
- Andersson K-E (2003) Erectile physiological and pathophysiological pathways involved in erectile dysfunction. *J Urol* 170(2S):S6–S14
- Andersson K-E (2011) Mechanisms of penile erection and basis for pharmacological treatment of erectile dysfunction. *Pharm Rev* 63(4):811–859
- Anthony TG, Reiter AK, Anthony JC, Kimball SR, Jefferson LS (2001) Deficiency of dietary EAA preferentially inhibits mRNA translation of ribosomal proteins in liver of meal-fed rats. *Am J Physiol-Endocrinol Metab* 281(3):E430–E439
- Anthony NG, Johnston BF, Khalaf AI, MacKay SP, Parkinson JA, Suckling CJ, Waigh RD (2004) Short lexitropsin that recognizes

- the DNA minor groove at 5'-ACTAGT-3': understanding the role of isopropyl-thiazole. *J Amer Chem Soc* 126(36):11338–11349
- Aslan M, Thornley-Brown D, Freeman BA (2000) Reactive species in sickle cell disease. *Ann NY Acad Sci* 899(1):375–391
- Atolani O, Olatunji GA (2016) Chemical composition, antioxidant and cytotoxicity potential of *Daniellia oliveri* (Rolfe) Hutch. & Dalz. *Turk J Pharm Sci* 13(1):41–46
- Atolani O, Omere J, Otuechere C, Adewuyi A (2012) Antioxidant and cytotoxicity effects of seed oils from edible fruits. *J Acute Dis* 1(2):130–134
- Atolani O, Olatunji GA, Fabiyi OA, Adeniji AJ, Ogbale OO (2013) Phytochemicals from *Kigelia pinnata* leaves show antioxidant and anticancer potential on human cancer cell line. *J Med Food* 16(10):878–885
- Azenabor A, Ekun AO, Akinloye O (2015) Impact of inflammation on male reproductive tract. *J Reprod Infert* 16(3):123–129
- Bagatini MD, dos Santos AA, Cardoso AM, Mânica A, Reschke CR, Carvalho FB (2018) The impact of purinergic system enzymes on noncommunicable, neurological, and degenerative diseases. *J Immun Res*. <https://doi.org/10.1155/2018/4892473>
- Berman H, Westbrook J, Feng Z, Gilliland G, Bhat T, Weissig H, Shindyalov I, Bourne P (2000) The protein data bank. *Nucl Acid Res* 28:235–242
- Brownlee M (2001) Biochemistry and molecular cell biology of diabetic complications. *Nature* 414(6865):813
- Burnstock G (2014) Purinergic signalling in the reproductive system in health and disease. *Purine Signal* 10(1):157–187
- Chan CXA, Khan AA, Choi JH, Ng CD, Cadeiras M, Deng M, Ping P (2013) Technology platform development for targeted plasma metabolites in human heart failure. *Clin Proteom* 10(1):7
- Chong J, Soufan O, Li C, Caraus I, Li S, Bourque G, Wishart DS, Xia J (2018) *MetaboAnalyst 4.0*: towards more transparent and integrative metabolomics analysis. *Nucl Acid Res* 46(W1):W486–W494
- Chougouo RDK, Nguekeu YMM, Dzoyem JP, Awouafack MD, Kouamou J, Tane P, McGaw LJ, Eloff JN (2016) Anti-inflammatory and acetylcholinesterase activity of extract, fractions and five compounds isolated from the leaves and twigs of *Artemisia annua* growing in Cameroon. *Springerplus* 5(1):1525
- Chowdhury P, Soulsby M (2002) Lipid peroxidation in rat brain is increased by simulated weightlessness and decreased by a soy-protein diet. *Ann Clin Lab Sci* 32(2):188–192
- Cojocar E, Filip N, Ungureanu C, Filip C, Danciu M (2014) Effects of valine and leucine on some antioxidant enzymes in hypercholesterolemic rats. *Health* 6(17):2313–2321
- Daina A, Michielin O, Zoete V (2017) SwissADME: a free web tool to evaluate pharmacokinetics, drug-likeness and medicinal chemistry friendliness of small molecules. *Sci Rep* 7:42717
- Drwal MN, Banerjee P, Dunkel M, Wettig MR, Preissner R (2014) ProTox: a web server for the in silico prediction of rodent oral toxicity. *Nucl Acid Res* 42(W1):W53–W58
- Du XL, Edelstein D, Dimmeler S, Ju Q, Sui C, Brownlee M (2001) Hyperglycemia inhibits endothelial nitric oxide synthase activity by posttranslational modification at the Akt site. *J Clin Invest* 108(9):1341–1348
- Ellman GL (1959) Tissue sulfhydryl groups. *Arch Biochem Biophys* 82(1):70–77
- Ellman GL, Courtney KD, Andres V Jr, Featherstone RM (1961) A new and rapid colorimetric determination of acetylcholinesterase activity. *Biochem Pharm* 7(2):88–95
- Erukainure O, Okafor O, Obode O, Ajayi A, Oluwale O, Oke O (2012) Blend of roselle calyx and selected fruit modulates testicular redox status and sperm quality of diabetic rats. *J Diab Metab* 3(214):2
- Erukainure OL, Mopuri R, Oyebo OA, Koorbanally NA, Islam MS (2017a) *Dacryodes edulis* enhances antioxidant activities, suppresses DNA fragmentation in oxidative pancreatic and hepatic injuries; and inhibits carbohydrate digestive enzymes linked to type 2 diabetes. *Biomed Pharmacother* 96:37–47
- Erukainure OL, Oyebo OA, Sokhela MK, Koorbanally NA, Islam MS (2017b) Caffeine-rich infusion from *Cola nitida* (kola nut) inhibits major carbohydrate catabolic enzymes; abates redox imbalance; and modulates oxidative dysregulated metabolic pathways and metabolites in Fe<sup>2+</sup>-induced hepatic toxicity. *Biomed Pharmacother* 96:1065–1074
- Erukainure OL, Hafizur R, Kabir N, Choudhary I, Atolani O, Banerjee P, Preissner R, Chukwuma CI, Muhammad A, Amonsou E (2018a) Suppressive effects of *clerodendrum volubile* P Beauv. [Labiatae] methanolic extract and its fractions on type 2 diabetes and its complications. *Front Pharm* 9:8. <https://doi.org/10.3389/fphar.2018.00008>
- Erukainure OL, Narainpersad N, Singh M, Olakunle S, Islam MS (2018b) *Clerodendrum volubile* inhibits key enzymes linked to type 2 diabetes but induces cytotoxicity in human embryonic kidney (HEK293) cells via exacerbated oxidative stress and proinflammation. *Biomed Pharmacother* 106:1144–1152
- Erukainure OL, Oyebo OA, Ibeji CU, Koorbanally NA, Islam MS (2019a) *Vernonia Amygdalina* Del. stimulated glucose uptake in brain tissues enhances antioxidative activities; and modulates functional chemistry and dysregulated metabolic pathways. *Metab Brain Dis* 34(3):721–732. <https://doi.org/10.1007/s11011-018-0363-7>
- Erukainure OL, Reddy R, Islam MS (2019b) *Raffia palm* (*Raphia hookeri*) wine extenuates redox imbalance and modulates activities of glycolytic and cholinergic enzymes in hyperglycemia induced testicular injury in type 2 diabetes rats. *J Food Biochem*. <https://doi.org/10.1111/jfbc.12764>
- Ezuruike UF, Prieto JM (2014) The use of plants in the traditional management of diabetes in Nigeria: pharmacological and toxicological considerations. *J Ethnopharm* 155(2):857–924
- Furtmüller PG, Obinger C, Hsuanyu Y, Dunford HB (2000) Mechanism of reaction of myeloperoxidase with hydrogen peroxide and chloride ion. *Euro J Biochem* 267(19):5858–5864
- Ge R-S, Dong Q, Sottas CM, Chen H, Zirkin BR, Hardy MP (2005) Gene expression in rat Leydig cells during development from the progenitor to adult stage: a cluster analysis. *Biol Reprod* 72(6):1405–1415
- Gorodeski GI (2015) Purinergic signalling in the reproductive system. *Auton Neurosci* 191:82–101
- Granell S, Gironella M, Bulbena O, Panes J, Mauri M, Sabater L, Aparisi L, Gelpi E, Closa D (2003) Heparin mobilizes xanthine oxidase and induces lung inflammation in acute pancreatitis. *Crit Care Med* 31(2):525–530
- Guazzone VA, Jacobo P, Theas MS, Lustig L (2009) Cytokines and chemokines in testicular inflammation: a brief review. *Microscop Res Tech* 72(8):620–628
- Gul K, Singh AK, Jabeen R (2016) Nutraceuticals and functional foods: the foods for the future world. *Crit Rev Food Sci Nutr* 56(16):2617–2627
- Habig WH, Pabst MJ, Jakoby WB (1974) Glutathione S-transferases the first enzymatic step in mercapturic acid formation. *J Biol Chem* 249(22):7130–7139
- Ham DJ, Caldwell MK, Lynch GS, Koopman R (2014) Leucine as a treatment for muscle wasting: a critical review. *Clin Nutr* 33(6):937–945
- Harman LS, Mottley C, Mason RP (1984) Free radical metabolites of L-cysteine oxidation. *J Biol Chem* 259(9):5606–5611
- Heymann D, Reddington M, Kreutzberg GW (1984) Subcellular localization of 5'-nucleotidase in rat brain. *J Neurochem* 43(4):971–978
- Homa ST, Vassiliou AM, Stone J, Killeen AP, Dawkins A, Xie J, Gould F, Ramsay JW (2019) A comparison between two assays for measuring seminal oxidative stress and their relationship with sperm DNA fragmentation and semen parameters. *Genes* 10(3):236

- Hsieh YY, Sun YL, Chang CC, Lee YS, Tsai HD, Lin CS (2002) Superoxide dismutase activities of spermatozoa and seminal plasma are not correlated with male infertility. *J Clin Lab Anal* 16(3):127–131
- Jones G, Willett P, Glen RC, Leach AR, Taylor R (1997) Development and validation of a genetic algorithm for flexible docking. *J Mol Biol* 267(3):727–748
- Kakkar P, Das B, Viswanathan P (1984) A modified spectrophotometric assay of superoxide dismutase. *Indian J Biochem Biophys* 21:130–132
- Kanias T, Acker JP (2010) Biopreservation of red blood cells—the struggle with hemoglobin oxidation. *FEBS J* 277(2):343–356
- Koeck T, Stuehr D, Aulak K (2005) Mitochondria and regulated tyrosine nitration. *Biochem Soc Transact* 33(6):1399–1403
- Lantum HB, Cornejo J, Pierce RH, Anders M (2003) Perturbation of maleylacetoacetic acid metabolism in rats with dichloroacetic acid-induced glutathione transferase zeta deficiency. *Toxicol Sci* 74(1):192–202
- Le Magueresse-Battistoni B (2007) Serine proteases and serine protease inhibitors in testicular physiology: the plasminogen activation system. *Reproduction* 134(6):721–729
- Leba L-J, Brunschwig C, Saout M, Martial K, Vulcain E, Bereau D, Robinson J-C (2014) Optimization of a DNA nicking assay to evaluate *Oenocarpus bataua* and *Camellia sinensis* antioxidant capacity. *Int J Mol Sci* 15(10):18023–18039
- Lee JH, Park E, Jin HJ, Lee Y, Choi SJ, Lee GW, Chang P-S, Paik H-D (2017) Anti-inflammatory and anti-genotoxic activity of branched chain amino acids (BCAA) in lipopolysaccharide (LPS) stimulated RAW 264.7 macrophages. *Food Sci Biotech* 26(5):1371–1377
- Li S-F, Liu H-X, Zhang Y-B, Yan Y-C, Li Y-P (2010) The protective effects of  $\alpha$ -ketoacids against oxidative stress on rat spermatozoa in vitro. *Asian J Androl* 12(2):247–256
- Lucas TSF, Avellar MCW, Porto CS (2004) Effects of carbachol on rat Sertoli cell proliferation and muscarinic acetylcholine receptors regulation: an in vitro study. *Life Sci* 75(14):1761–1773
- Luo Y, Han Z, Chin SM, Linn S (1994) Three chemically distinct types of oxidants formed by iron-mediated Fenton reactions in the presence of DNA. *Proceed Nat Acad Sci* 91(26):12438–12442
- Melo JB, Agostinho P, Oliveira CR (2003) Involvement of oxidative stress in the enhancement of acetylcholinesterase activity induced by amyloid beta-peptide. *Neurosci Res* 45(1):117–127
- Mor I, Soreq H (2011) Cholinergic toxicity and the male reproductive system. In: *Reproductive and developmental toxicology*. Elsevier, Amsterdam, pp 863–870
- Mruk DD, Silvestrini B, Mo M-y, Cheng CY (2002) Antioxidant superoxide dismutase—a review: its function, regulation in the testis, and role in male fertility☆. *Contraception* 65(4):305–311
- Nicastro H, Da Luz CR, Chaves DFS, Bechara LRG, Voltarelli VA, Rogero MM, Lancha AH (2012) Does branched-chain amino acids supplementation modulate skeletal muscle remodeling through inflammation modulation? Possible mechanisms of action. *J Nutr Metab* 2012:1
- Nicastro H, Carvalho M, Barquilha G, Ferreira LS (2017) Leucine supplementation: a possible anti-inflammatory strategy evidences from a pilot study. *Age (years)* 24(1.2):21–20
- Obode O, Okafor O, Erukainure O, Ajayi A, Suberu Y, Ogunji A, Okporua T, Oluwole O, Ozumba A, Elemo G (2015) Protective effect of some selected fruit blends on testicular toxicity in alloxan-induced diabetic rats. *J Compl Integr Med* 12(2):137–142
- Osunsanmi FO, Zharare GE, Mosa RA, Ikhile MI, Shode FO, Opoku AR (2019) Anti-oxidant, anti-inflammatory and antiacetylcholinesterase activity of betulinic acid and 3 $\beta$ -acetoxybetulinic acid from *Melaleuca bracteata* ‘Revolution Gold.’ *Trop J Pharm Res* 18(2):303–309
- Panner Selvam M, Agarwal A, Sharma R, Samanta L (2018) Treatment of semen samples with  $\alpha$ -chymotrypsin alters the expression pattern of sperm functional proteins—a pilot study. *Andrology* 6(2):345–350
- Pedroso J, Zampieri T, Donato J (2015) Reviewing the effects of L-leucine supplementation in the regulation of food intake, energy balance, and glucose homeostasis. *Nutrients* 7(5):3914–3937
- Reddy MM, Mahipal SV, Subhashini J, Reddy MC, Roy KR, Reddy GV, Reddy PR, Reddanna P (2006) Bacterial lipopolysaccharide-induced oxidative stress in the impairment of steroidogenesis and spermatogenesis in rats. *Reprod Toxicol* 22(3):493–500
- Salau VF, Erukainure OL, Ayeni G, Ibeji CU, Islam MS (2020) Modulatory effect of ursolic acid on neurodegenerative activities in oxidative brain injury: an ex vivo study. *J Food Biochem*. <https://doi.org/10.1111/jfbc.13597>
- Saleem H, Ahmad I, Ashraf M, Gill MSA, Nadeem MF, Shahid MN, Barkat K (2016) In vitro studies on anti-diabetic and anti-ulcer potentials of *Jatropha gossypifolia* (Euphorbiaceae). *Trop J Pharm Res* 15(1):121–125
- Salles M, Viana F, Van De Meent M, Rhee I, Verpoorte R (2003) Screening for acetylcholinesterase inhibitors from plants to treat Alzheimer disease. *Química Nova* 26:1–7
- Saxena R, Pendse V, Khanna N (1984) Anti-inflammatory and analgesic properties of four amino-acids. *Indian J Physiol Pharm* 28(4):299–305
- Schetteringer MRC, Morsch VM, Bonan CD, Wyse AT (2007) NTPDase and 5'-nucleotidase activities in physiological and disease conditions: new perspectives for human health. *BioFactors* 31(2):77–98
- Shukla A, Mishra R, Pandey A, Dwivedi A, Kumar D Interaction of Flavonols with DNA: Molecular Docking Studies. In: *Proceed Inter Symp Adv Funct Biol Mater (ISAFBM-2019)*, 2019. p 4
- Tourmente M, Villar-Moya P, Rial E, Roldan ER (2015) Differences in ATP generation via glycolysis and oxidative phosphorylation and relationships with sperm motility in mouse species. *J Biol Chem* 290(33):20613–20626
- Velarde MC (2014) Mitochondrial and sex steroid hormone crosstalk during aging. *Longev Healthspan* 3(1):2
- Wishart DS, Jewison T, Guo AC, Wilson M, Knox C, Liu Y, Djoumbou Y, Mandal R, Aziat F, Dong E, Bouatra S, Sinelnikov I, Arndt D, Xia J, Liu P, Yallou F, Bjorn Dahl T, Perez-Pineiro R, Eisner R, Allen F, Neveu V, Greiner R, Scalbert A (2013) HMDB 3.0—the human metabolome database in 2013. *Nucl Acid Res* 41(D1):D801–D807. <https://doi.org/10.1093/nar/gks1065>
- Yang J, Chi Y, Burkhardt BR, Guan Y, Wolf BA (2010) Leucine metabolism in regulation of insulin secretion from pancreatic beta cells. *Nutr Rev* 68(5):270–279

**Publisher's Note** Springer Nature remains neutral with regard to jurisdictional claims in published maps and institutional affiliations.